Traceable digital twin for accurate positioning of industrial robot arms in human–robot collaborative systems

Flexible Services and Manufacturing Journal
https://doi.org/10.1007/s10696-025-09632-7

Traceable digital twin for accurate positioning of industrial robot arms in human–robot collaborative systems

Giacomo Maculotti[1] · Fazluddin Khusnuddinov[2] · Jasurkhuja Kholkhujaev[1,2] · Gianfranco Genta[1] · Maurizio Galetto[1]

Accepted: 22 June 2025

Abstract

Human–robot collaborative (HRC) systems are getting increasing attention of researchers and industry due to their flexibility allowing high-level customization of manufacturing process. However, shared workspace between operators and robots constrains to use specialized industrial robots known as collaborative robots or cobots that have a limited speed and payload characteristics, which are still liable of inducing systematic errors in the positions. The position control of cobots during the design, validation and operation phase is crucial for the human operators' safety and secure operation to avoid contact with the operator or the surrounding environment, liable of causing damages, as well as for avoiding unnecessary adjustments of the workspace. This work discusses the application of a machine learning-based Digital Twin (DT) including online position correction and error prediction method for HRC systems to allow safe operators' training and planning of collaborative tasks. Innovatively, a metrologically trustworthy DT is introduced by including calibration of the models and evaluating and propagating the measurement uncertainty of error correction model. The proposed procedure is demonstrated on a state-of-the-art Yaskawa cobot, showing an improvement of positioning precision from 0.970 to 0.216 mm, i.e., of 77.8%.

Keywords Digital twin · Measurement uncertainty · Human–Robot collaboration · Robotics · Position correction

✉ Giacomo Maculotti
giacomo.maculotti@polito.it

[1] Department of Management and Production Engineering, Politecnico di Torino, Corso Duca degli Abruzzi 24, 10129 Turin, Italy

[2] Turin Polytechnic University in Tashkent, Kichik Halka Yuli, 17, Tashkent, Uzbekistan

Published online: 05 August 2025

1 Introduction

In the last decades, high production rates, increased product variability and on-going industrial revolution are requiring manufacturing to be more adaptive, customizable, accurate and fast (Khan and Turowski 2016; Yin et al. 2018). Manufacturers are shifting from mass production systems to flexible and customizable production processes to meet the customer demand. The future production systems will have to cope with individualization of products that should be ready to ship from conveyors of high quality. Evolution of Industry 4.0 paradigm significantly advanced the manufacturing technologies, production processes and quality control systems (B. Chen et al. 2018; Foidl and Felderer 2016; Michael Rüßmann et al. 2015; Salkin et al. 2018). A new paradigm came with a number of innovative technologies i.e. Internet of things (IoT), Big Data, cloud computing, cyber-physical systems (Lindström et al. 2019). The objective of Industry 4.0 is to increase the quality, productivity and to reduce cost through close integration of automation systems. This has led to the increased use of industrial robots in various application like welding, material handling, assembly, surface characterization and non-contact measurements (Maculotti et al. 2021; Kholkhujaev et al. 2022; Oztemel and Gursev 2020). Due to high reliability and speed of industrial robots, today, they are integral part of production systems.

However, in some industries and industrial applications the manufacturers still rely on humans to accomplish tasks that require flexibility, fast adaptation into unpredicted situations and assembly of complex geometries. A novel technology has been evolved known as collaborative robots or cobots aiming to safely share the tasks and workspace with humans (Peshkin and Colgate 1999). Generally, cobots have lower speed and payloads to reduce hazards for human operators. Cobots should comply with ISO/TS 15066 standard on safety (ISO/TS 15066:2016) Collaborative robots (2016). Collaborative robots and human interaction can be classified according to task allocation and workspace sharing (Saravanan et al. 2020) and symbiotic interactions (Barravecchia et al. 2023a, b). Cobots enabled direct interaction between humans and robots thus taking advantage of cognitive skills of humans and high repeatability of robots in the shop floors as shown in Fig. 1. Thus, sharing the environment brings a wide set of advantages i.e., combining the skills of the human with robot which brought back at the core of industry the figure of human operator within the framework of Industry 5.0 (Verna et al. 2023b). This leads to increased productivity of operators (Barravecchia et al. 2023a, b) and decrease of stress-fatiguing of humans(Gervasi et al. 2022).

Additionally, the other key influencing factor for integration of collaborative systems is that they can be programmed and taught in rather straightforward and intuitive ways compared to traditional industrial robot programming (Billard et al. 2016). Researchers developed several cobot teaching algorithms that are based on virtual reality, augment reality, demonstrative programming (Lambrecht et al. 2013) and gesture recognition-based teaching (Brugali et al. 2014). On the contrary, the traditional industrial robot programming requires high level professionals due to safety concerns in workspace. Safety concerns still play an important role in the design of human–robot shared workspaces. Human–robot collaboration (HRC) systems mainly focus on processes with high diversity of products and where dexterity on

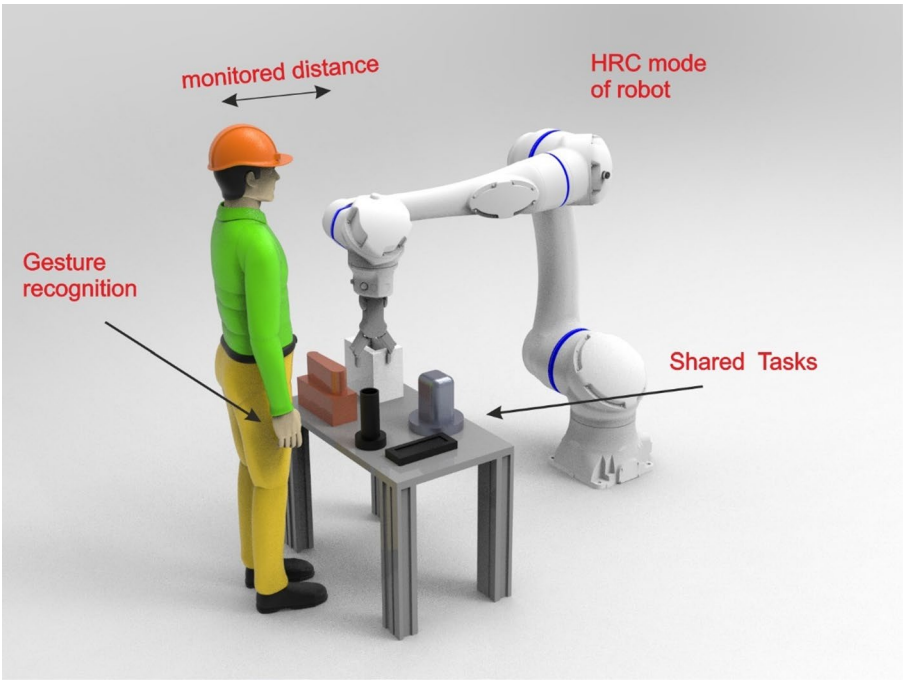

Fig. 1 Human–robot collaborative workspace (Gervasi et al. 2020)

the assembly of complex geometries is important (Verna et al. 2023c). Safety concerns, complex task allocation and shared workspace creates additional difficulties for design of HRC systems as can be seen in Fig. 1 (Lindström et al. 2019). They are generally characterized by frequent change of production processes and customization that necessitates the HRC design phase to be validated and updated quickly before applying into the real world. Traditional methods of validation and design are time-consuming and require heavy computation effort (Tsarouchi et al. 2017).

Fu et al. (2020) observed that in real production environments there are relatively large differences between the actual and programmed positions of the robots. Gear transmission errors, spatial orientation errors, serial kinematic structure errors and compliance errors due to external forces may cause large and significant positioning error (Liu et al. 2022; Song et al. 2022). Additionally, extensive use of robots, wear and aging is another factor influencing the increase of positioning errors. According to Li et al. (Li et al. 2021), positioning errors can be classified into geometric parameter errors that are direct result of the structure of the robots and non-geometric parameter errors that are caused by friction, external forces and temperature. Therefore, the position control of cobots is of vital importance during the design of HRC workspaces that could prevent serious accidents or predict unexpected situations. In the following subsections, an introductory focus will be given on position error identification and management of industrial robots and on Digital Twin of robotic arms.

1.1 Industrial robot position error correction

According to the International Vocabulary of Metrology (VIM) (JCGM 200:2012) a systematic error can be corrected by means of the application of a compensation measure, which can either be a numerical correction or a physical modification of the system. Literature often uses correction and compensation terms as synonyms; in the following we will discuss error correction strategies attaining to the terminology introduced in the original papers. The position error compensation methods can be classified into kinematic model-based methods and direct error mapping methods (Cho et al. 2019; Gan et al. 2019; Lattanzi et al. 2020; Santolaria et al. 2013; Zhao et al. 2016). Kinematic model-based approaches mainly focus on finding deterministic relationships between the joint angles and pose errors. Denavit-Hartenberg (D-H) is a traditional robot kinematic model (Gan et al. 2019), together with Product of Exponentials (POE) and Stones models (Cho et al. 2019; Wu et al. 2015) that are fundamental approaches to establish kinematic model-based error compensation. Based on classical kinematic models of the robots, Song et al. (2022) developed a model that uses finite and instantaneous screw (FIS) theory propagating geometric and deformation errors separately. The analysis concluded that pose errors result from the superposition of joint deflection and geometric errors. Cho et al. (2019) considering that the traditional POE does not include the joint deflections proposed a modified POE model. Similarly, compliance model-based approach calibrated by laser tracker for correcting the systematic positioning errors of robot were considered (Chancharoen et al. 2022; Gonzalez et al. 2022; Posada et al. 2016). It was found that the analytical model-based error correction does not completely eliminate the process dependent errors, and external sensor-based compensation yields generally better results.

Many of the above methods partially or fully do not consider non geometric errors e.g., temperature, external forces, external vibrations. Hence, the utilization of those models within the real production environment or for diverse tasks might result in failure or inefficiency of the system. Kinematic-based approaches necessitate high level expertise and knowledge that makes the model challenging (Zhou et al. 2023).

On the contrary, the direct mapping of target and actual positions are mostly done based on neural networks or machine learning (ML) algorithm, that helps directly quantify and compensate the systematic error. Chen et al. (2019) and Shanghai et al. (2021) used back propagation (BP) neural network algorithm to compensate the absolute positioning error. Stiffness based data was used as an input and theoretical target coordinates as an output data to train the model, however the metrological assessment has not been performed and stiffness is assumed as the most influencing non-geometric parameter. Gao et al. (2017) proposed BP neural network model with initial input dataset generated by Monte-Carlo method to evaluate the errors on articulated coordinate measurement machine. Wu et al. (2018) applied an Adaptive Neuro-fuzzy Inference System (ANFIS) for joint error compensation, resulting in a powerful method to handle non-linear relations between input and output datasets. Wang et al. (2005) developed a neural network-based pose calibration method attaching calibrated camera on the end-effector. The actual position was evaluated by camera on the end-effector. The neural network model was developed based on the position errors as outputs and target positions as inputs. The prediction was done

for unknown target positions. Bilal et al. (2022) also proposed camera-laser based position error estimation method that used Levenberg–Marquardt (LM) algorithm to evaluate the kinematic parameters of robot. A laser tracker was used to decrease the errors due to the positioning of the camera and markers. Long Short-Term Memory (LSTM) was applied to extract the dynamic characteristics of system that was later fed into sparse regression neural network model to increase the accuracy of pose estimation. Other researchers applied various optical calibration methods for error compensation with integration of neural network algorithms (Shu et al. 2018). Zhou et al. (2023) applied adaptive hierarchical compensation model for error compensation and optimization of pose mapping model. The algorithm uses fixed-length incremental model (FIL) to optimize the model parameters and incremental model reconstruction (IMR) to enhance the model architecture. There are also hybrid approaches that model kinematics of industrial robot using both analytical and statistical methods. Nguyen and Marvel (2022) implemented analytical Forward and Inverse Kinematics method as a prior mean function for Gaussian process and Bayesian inference is further used to update Gaussian process model. Furthermore, the work also compares the error propagation of robot kinematics modeling methods i.e. analytical, no-prior, neural network and hybrid models.

1.2 Digital twin of robotic arms

Recently, advancements of virtualization and digitalization of manufacturing along with increased affordability of real-time data acquisition sensors supported the development of Digital Twin (DT) (Tao et al. 2018). The DT technology was first implemented in the NASA's Apollo program that developed two identical spacecrafts (Rosen et al. 2015). The purpose of the earth-based twin was to simulate and mirror the flight behavior during the Apollo mission. This helped the engineers to predict a critical situation and assist astronauts. Thus, any system having a counterpart that mirrors the real time behavior could be seen as a digital twin. However, there are several definitions among the researchers. Digital Twin concept was first presented in the context of production life-cycle management (PLM) in 2003 by Grieves (He and Bai 2021). The idea behind the DTs development was the possibility of having physical and virtual entities that contain all the data within their own domains. The bi-directional automatic data exchange of physical entities with the digital counterparts can help to develop efficient products and services.

DT is defined as a system with continuous automatic exchange of data between virtual and physical entities as in the Fig. 2 (Errandonea et al. 2020; ISO 23247-1:2021). DT was developed to comply with complex production systems that should be quickly able to adapt to changes with great focus on product customization, product quality and decentralization of production facilities (Verna et al. 2023a). Flexibility and complexity are the two challenging characteristics of the human and robot shared workspaces. Therefore, the integration of DT systems in HRC production is getting increased attention by researchers (Jones et al. 2020; Tao et al. 2018). Wilhelm et al. (2020) proposed an adaptive automation model to combine an optimize the productivity of operators and machines in container unloading process. Oyekan et al. (2019) used DT for modelling human reaction to predictable and unpredictable

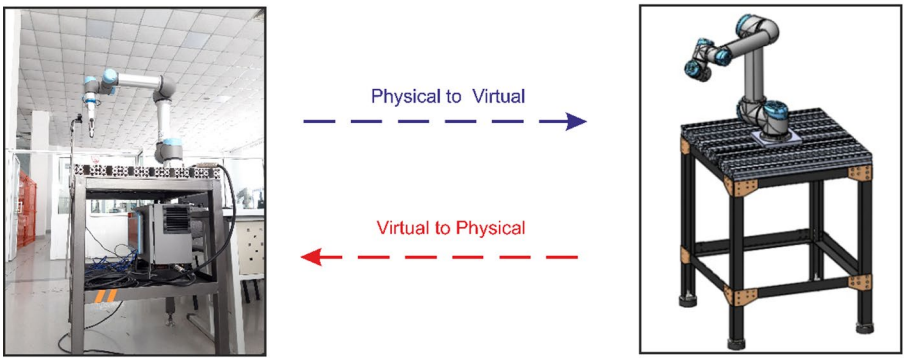

Fig. 2 Digital twin layout with automatic data exchange between physical to virtual and virtual to physical entities

cobot movements. Kinetic Energy ratio approach was implemented to evaluate and validate virtual reality environment. Sanderud et al. developed risk field approach for constantly reducing the risk for operators in HRC systems (Sanderud et al. 2015).

Wu et al. (2022) proposed low-cost attitude sensor-based error compensation method for articulated robot arms that establishes virtual-physical interaction between real and digital systems. Pottier et al. (2023) proposed a multi-camera metrology-based method to evaluate possibility of developing DT systems for robotic environments. Their research used Blender as a virtual environment and found that it lacks the "realism" and has poor accuracy compared to real world pose estimation results. Zhang et al. (2022) developed DT environment with online Gaussian Process (GP) based control model to predict the seam positions for welding process aided by the use of a machine vision system (MVS). A number of researchers focused on monitoring and optimization of the path of robotic and automated systems (Li et al. 2021; Shu et al. 2018; Song et al. 2022). Slavkovic et al. (2020) proposed a DT system for the correction of end-effector trajectory for milling robots that is based on analytical kinematic model of a robot. Numerical simulation-based DT were also implemented to improve the accuracy of the physical systems (Irino et al. 2023; Luo et al. 2020). However, physics-based simulation models that require a numerical method cannot always be applied in high-rate production processes where the real-time control is of importance due to the long computational time, and often surrogate models are resorted to, most modeled by GP, or hybrid models are resorted to (Zhu et al. 2023).

However, as summarized in Table 1, despite the use of machine learning methods, and the adoption of—sometimes traceable—calibration approaches to estimate and correct the errors, one substantial lack in the literature is tying the prediction and consequent correction to its measurement uncertainty. In fact, without a metrological framework to cater for all the relevant contributions arising from sensors, actuators and the stochastic control algorithm, closed loop feedback control and simulation typical of DTs applications will lack the required confidence for users.

Bilberg and Malik (2019) pointed out the importance of integrating DTs in the HRC systems analyzing the HRC linear actuators line. It was highlighted that DTs can support HRC systems in automation while remaining flexible in assembly. How-

Table 1 Main error correction methods for robot arm positioning performance

Reference	Industrial System	DT	Traceable	Uncertainty	Modelling strategy	Error as is	Error after correction
Wu et al. (2015)	ABB IRB120	No	Yes	No	Kinematic propagation of exponential model	Position error (18.17 ± 13.39) mm	Position error (0.79 ± 0.71) mm
Posada et al. (2016)	Kuka KR210	No	Yes	No	Kinematic model compensated for compliance	Average position error 2.75 mm	Average position error 0.3 mm
Wu et al. (2018)	EAST Articulated Maintenance Arm	No	No	No	Adaptive neuro-fuzzy inference	Average elevation angle error 0.02°	Average elevation angle error 0.01°
Cho et al. (2019)	TX60	No	Yes	No	Kinematic models–propagation of exponential	Residual position error (conventional circular point analysis) (0.8 ± 0.58) mm	Residual position error (0.5 ± 0.46) mm
	AMIRO					Residual position error (conventional Circular Point Analysis) (12 ± 11.6) mm	Residual position error (8 ± 4.6) mm
Gan et al. (2019)	EFORT ER3A	No	Yes	No	Kinematic model	Position error (3.84 ± 1.73) mm	Position error (1.39 ± 1.16) mm
Lattanzi et al. (2020)	DENSO VS-087	No	Yes	No	Circular point analysis	Position error (1 ± 1.16) mm	Position error (0.06 ± 0.046) mm
Bilal et al. (2022)	KUKA KR240 R2900	No	Yes	No	MVS tracking and NN	Residual position error (conventional Kalman filer control) 5.47 mm	Position error 2.9 mm
Song et al. (2022)	Universal Robot UR3	No	Yes	No	Kinematic model	Position error (9.24 ± 5.77) mm	Position error (0.30 ± 0.23) mm

Table 1 (continued)

Reference	Industrial System	DT	Traceable	Uncertainty	Modelling strategy	Error as is	Error after correction
Slavkovic et al. (2020)	Robot arm machine tool	Yes	No	No	Kinematic model and cutting force analysis	Position error (0.25 ± 0.058) mm	Position error (0.025 ± 0.058) mm
Shanghai et al. (2021)	Ningbo Weili Robot Technology	No	Yes	No	PBNN	Average position error 0.591 mm	Average position error 0.115 mm
Chancharoen et al. (2022)	Universal Robot UR3	Yes	No	No	Kinematic model (embedded in commercial simulator)	Unreported	Position Error RMSE 2 mm
Gonzalez et al. (2022)	COMAU AURA	Yes	Yes	No	Kinematic model with compliance compensation	Position error (0.6 ± 0.29) mm	Position error (0.3 ± 0.29) mm
Wu et al. (2022)	Anno Robot J601	Yes	No	No	Numerical linear model	Orientation angle error (joint L) 0.15°	Orientation angle error (joint L) 0.008°
Zhang et al. (2022)	Robot arm Laser welding system	Yes	No	No	MVS and GPR	Residual Position error (conventional PID controller) (0.085 ± 0.226) mm	Position error (0.039 ± 0.164) mm
Zhu et al. (2023)	Stäubli TX200	Yes	No	No	Hybrid Machine Learning	Average Position error 0.85 mm	Average Position error 0.13 mm
	UR10 CB3					Average Position error 2.11 mm	Average Position error 0.17 mm

Highlight of Digital Twin, uncertainty and traceability of implementation. Error dispersion, when available, has been reported as confidence interval at 95% confidence level, calculated from the half-range variability reported in the reference as Type B contribution, assuming a uniform distribution

ever, the mentioned applications of DTs in industrial and collaborative robots have shown a lack of metrological characterization and measurement uncertainty propagation. This is essential to enable a holistic and conservative comparison of different approaches, and to enable verification of tolerances and design of applications within a metrological and statistical framework, to elicit a safe collaborative working environment.

The present paper effectively utilizes the concept of HRC systems and proposes the method to safe operation of humans and robots developing DT model-based approach to predict and detect the position error of the cobot. In particular, the simulation of the path will include measurement uncertainty of the actuators and the correction control algorithm such that the training and path planning can take place catering for uncertainty of the system increasing the reliability and the safety of use.

In this paper, a digital environment of the collaborative robot is developed in a virtual simulation environment. A multi-camera tracking system is used to collect the data on the end-effector of the cobot. A laser tracker is used to calibrate the position systematic errors model based on a machine learning Gaussian Process Regression (GPR). The calibration will ensure the traceability of the DT. The GPR correction-based method is proposed to predict and detect the positioning errors of the system including kinematic and dynamic errors and compliance induced errors. As highlighted in the literature, this avoids complex and computationally intensive physics-based modelling and the solution of the inverse kinematics. To ensure the statistical significance of the GPR correction- model and the DT, and to evaluate metrological characteristics of DT, the propagation of uncertainty is considered to provide a metrological performance evaluation in the DT framework.

The rest of the paper is organized as follows. Section 2 presents the methodology used to model the DT system with particular focus on DT-driven HRC systems, GPR modelling, and data acquisition. Section 3 discusses the results and findings of the GPR model-based positioning error estimation. Finally, Sect. 4 draws conclusions from the findings.

2 Methodology

This work aims to predict and correct the position error of a collaborative robot based on DT model of the system. GPR model for mapping the position error by means of a surrogate model is proposed. Figure 3 shows a general overview of proposed GPR model-based DT system that corrects the positioning error and suggests when it is necessary to send the cobot for maintenance. The algorithm consists of Virtual entity and Physical entity of the cobot with feedback control loop that aims at correcting systematic error and control when errors larger than the prediction are generated, i.e. out-of-control positioning. The triangular hat on the quantities represents GPR trained models' estimation, while quantities in bold are vectors.

In the case at hand, a typical tool center point (TCP) position-programming is considered. This consists in programming the robot arm by specifying the TCP position $\boldsymbol{TCP} = \{x_{TCP}, y_{TCP}, z_{TCP}\}$ in cartesian coordinates, as a function of some motion parameters $\boldsymbol{\theta}$, e.g. the motion speed $\boldsymbol{v} = \{v_x, v_y, v_z\}$(most commonly

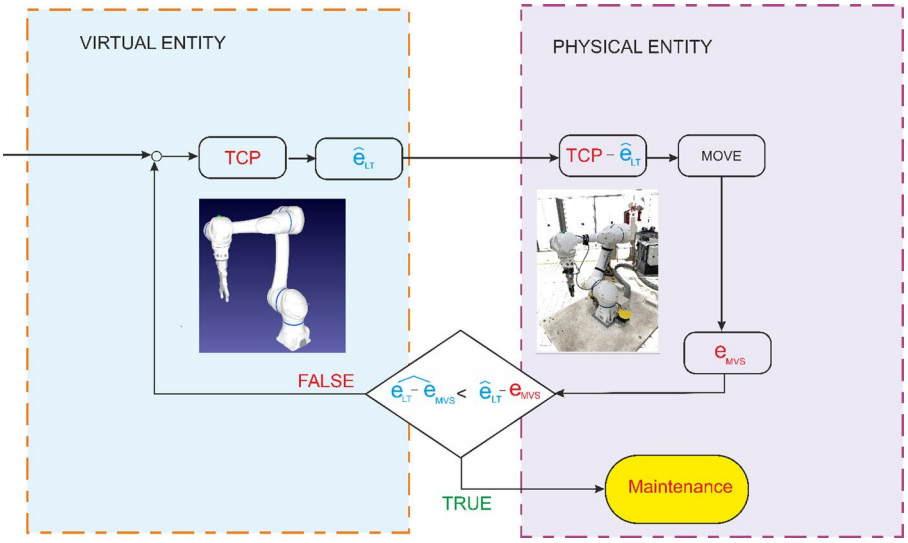

Fig. 3 Proposed DT based error prediction and detection method

expressed in magnitude v), the type of motion (either linear of joint). However, as reviewed in the literature, due to kinematic, dynamic and finite stiffness, a position error $\boldsymbol{e}$ results, which is typically systematic, and is a function of the cartesian coordinate (due to kinematics and compliance-related errors) and the motion parameters, which are associated to the dynamics of the system, so that $\boldsymbol{e} = \boldsymbol{f}(\boldsymbol{TCP}, \boldsymbol{\theta})$. Robot axes calibration performed by laser tracker (LT), according to state-of-the-art literature (Zhou et al. 2023), allows estimating the error, $\widehat{\boldsymbol{e_{LT}}}$, which can be then exploited to correct the command, i.e. $\boldsymbol{TCP_c} = \boldsymbol{TCP} - \widehat{\boldsymbol{e_{LT}}}$, to improve positioning accuracy. A DT requires a dynamic update of both the physical and virtual entity (Maculotti et al. 2024). A convenient way relies on the use of exteroceptive sensor aimed at sensing the actual current state of the physical entity and updates the virtual counterpart accordingly. In the present work, a machine vision system (MVS) will be exploited consisting of eight cameras. Although in principle the laser tracker technology can be exploited as exteroceptive sensor, in actual application it would be highly impractical. In fact, the laser tracker severely limits the motion of the robot and the interaction in the working environment due to the need of a continuous optical connection between the laser source and the spherical mounted retroreflector (SMR). Moreover, the exteroceptive sensor can be exploited to detect anomalies, i.e. out-of-control position, which might be early indicators of the need of maintenance. This can rely on the positioning error calibration which can also be performed concurrently relying on the MVS, i.e. obtaining $\widehat{\boldsymbol{e_{MVS}}}$. The estimated residuals error and the real-time measured error $\boldsymbol{e_{MVS}}$ can be compared with the estimated residual errors from the laser tracker calibration to highlight such a condition. Indeed, such comparison shall be performed catering for uncertainty contribution to identify only statistically significant deviations, aspect currently missing in the literature that will be developed in Sect. 2.5 and will allow the establishment of a traceable DT for accurate TCP positioning.

2.1 Data acquisition

Two main hardware systems were used to acquire the position data of a state-of-the-art cobot Yaskawa MOTOMAN HC20DTP with maximum payload of 20 kg. The cobot is a 6-joints arm robot, with a maximum working distance of 1.9 m and a nominal positioning reproducibility of 50 µm, and a resolution of 1 µm. A large-scale 3D position measurement infrared camera system, namely an OptiTrack Prime^x 22 (resolution of 5 µm)and a laser tracker API R-20 Radian were used to model the DT system. The measurement systems were calibrated, resulting in an accuracy of 0.2 mm and an expanded uncertainty of 20 µm + 0.04 · L µm/m (where L is the measurement length expressed in meters), respectively for the OptiTrack and the laser tracker.

Position estimation of the cobot from the laser tracker (LT) was done attaching a spherical mounted retroreflector (SMR) on the OnRobot RG6 gripper as shown in Fig. 4. Absolute distance measurement (ADM) laser tracker measures and tracks the radial distance d_{LT} till SMR, together with two angles γ_{LT} and θ_{LT} that represent azimuth and elevation angle measurements respective (Franceschini et al. 2011). Distance and two angles are the 3 spherical coordinates that can be converted into cartesian coordinate frame. The measurement from LT is implemented offline for calibration purposes and does not necessitate real-time data acquisition during the real-time applications of proposed DT.

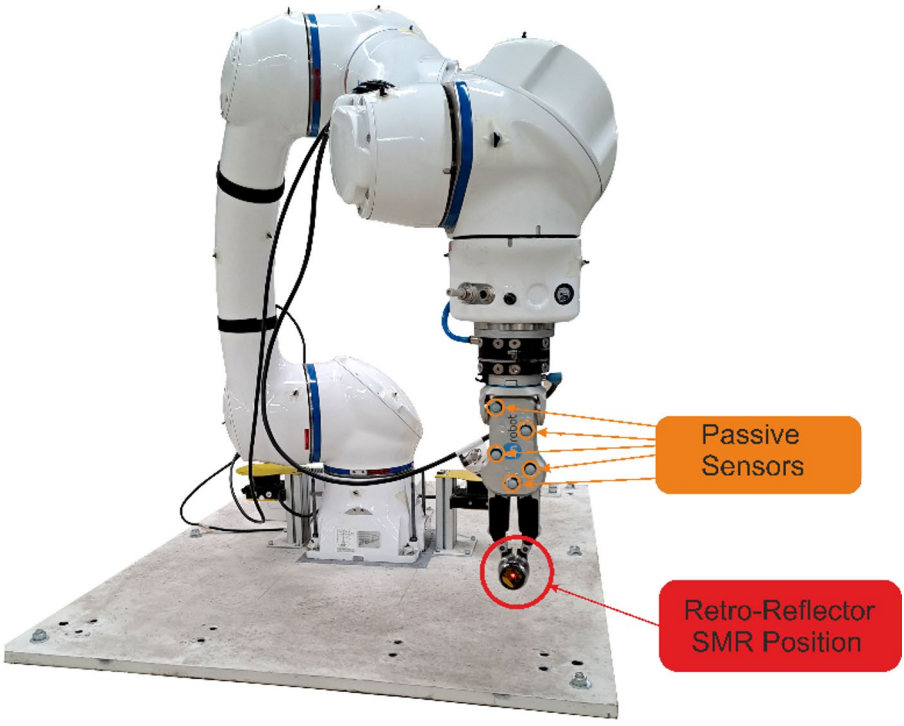

Fig. 4 Retroreflector of the LT and Passive Sensors to measure the position

Data acquisition from OptiTrack camera is performed by attaching 5 passive sensors on the surface of the gripper that are in constant offset with the SMR. Commercial software Motive (OptiTrack—Motive—In Depth 2023) is used to track the passive sensor coordinates. Five passive sensors shown in Fig. 4 are used to create coordinate system in Motive with the closest one to SMR as origin. The working area of the OptiTrack camera system enabled the tracking of the maximum reach of the cobot equal 1900 mm. To control the robot, MATLAB was used to send the coordinates through RoboDK simulator, and NatNet software development kit (SDK) was used to acquire passive sensor data from cameras. Ethernet connections are used to connect collaborative robot controller and Optitrack system into the laboratory computer, equipped with Intel Core i9 CPU and 128 GB of RAM.

2.2 Experimental methodology

The cobot is tested in Mind4Lab (Manufacturing for Industry 4.0 Laboratory) at the Department of Management and Production Engineering of Politecnico di Torino. The experimental procedure consists of three phases of data collection:

1. **Homogeneous transformation evaluation.** Dataset consisting of 12 points with 10 repetitions at maximum speed of cobot for evaluating the homogeneous transformation matrices which will be described in Sect. 2.3.
2. **GPR model training phase.** This phase is based on a Design of Experiments (DOE) approach. 62 target points are measured to train the GPR model and are shown in Fig. 5, where target points are chosen on the sides and the diagonals of rectangles with interval between the targets equal to 150 mm. Additional points

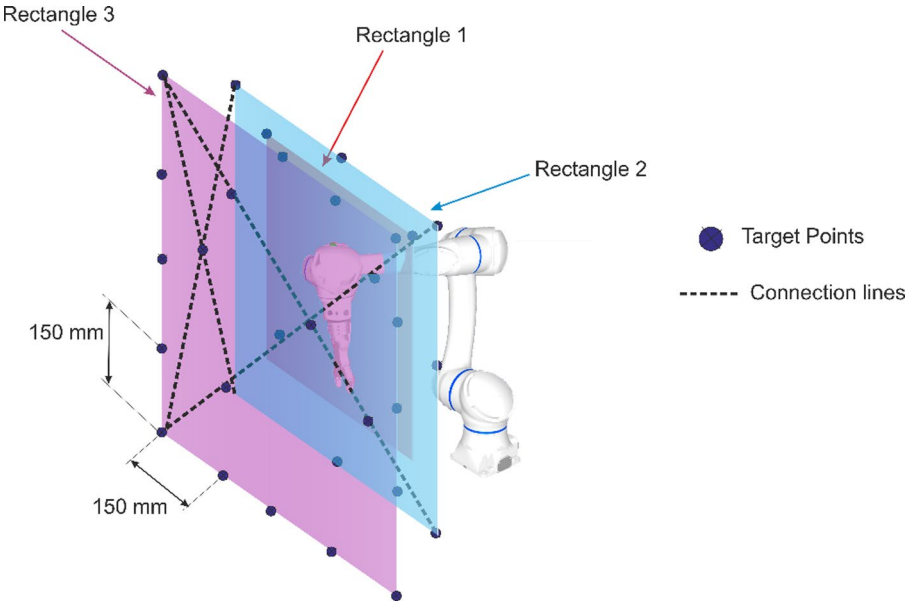

Fig. 5 DOE target points use to train GPR model

are taken on the lines connecting the vertexes of the rectangles. The planes are three rectangles with ascending areas are parallel and separated by 350 mm. Rectangle 1, Rectangle 2 and Rectangle 3 has 9, 13 and 26 target points respectively, with the rest 14 target points being on the connecting lines between rectangles' vertexes. Three different speed levels (v) that are 90%, 60% and 30% of the maximum speed of the cobot and only one type of motion was considered, i.e. linear motion. To acquire optimal parameters and avoid systematic influence due to the path and movement of the robot, the path is randomized and 9 replications (each of which with a different random path) are performed. This second phase of experiment is used to train and validate the GPR surrogate model. The GPR is selected according to the literature (as reviewed in Sect. 1.1) to allow a convenient mapping of positioning error capable at once of catering for kinematic, dynamic and compliance error (Rasmussen 2003). Furthermore, the GPR introduces the spatial covariance dependence in the error map, which is physically consistent with compliance-induced error (Mahler et al. 2014)

3. **Validation.** Test dataset consists of 14 target points with 5 replications at a speed of 80% and 5 replications at speed of 40% to validate GPR model is performed. Also, the same dataset is used to test the proposed method for closed-loop control of the cobot.

The implementation of the experiment for the registration matrix estimation, the DOE and the validation dataset took about 8 h. Programming of the cobot is implemented in cartesian coordinates in the RoboDK environment using a linear motion controlled by MATLAB.

2.3 Rigid body transformation

The measurement of the cobot position is performed by proprioceptive sensors, i.e. the cobot axes encoders, and two different exteroceptive sensors, i.e. the laser tracker and the OptiTrack system. Therefore, each measured TCP location is expressed in three local coordinate frames, and registration is needed to express then in one arbitrarily set global coordinate reference frame.

Let us consider a rigid body position evaluated in two different reference frames, i.e. $\boldsymbol{p_{LT}}$ in the coordinate system of the LT and $\boldsymbol{p_{GL}}$ in the global coordinate reference frame of GL. From the perspective of the two coordinate frames both the points can be related to each other, and there exist a rigid transformation T_{LT}^{GL} or T_{GL}^{LT} such that:

$$\forall \boldsymbol{p_{LT}}, \exists \boldsymbol{p_{GL}} : \| T_{LT}^{GL} \boldsymbol{p_{LT}} - \boldsymbol{p_{GL}} \| = 0 \tag{1}$$

$$\forall \boldsymbol{p_{GL}}, \exists \boldsymbol{p_{LT}} : \| T_{GL}^{LT} \boldsymbol{p_{GL}} - \boldsymbol{p_{LT}} \| = 0 \tag{2}$$

where $T_{LT}^{GL} \boldsymbol{p_{LT}}$ and $T_{GL}^{LT} \boldsymbol{p_{GL}}$ are the application of the transformation on $\boldsymbol{p_{LT}}$ and $\boldsymbol{p_{GL}}$ to bring them into the coordinate system of GL and LT, respectively. Any homogeneous transformation T_a^b can be represented having a component of rotation and translation, such that:

$$T_a^b = T\left(\alpha, \beta, \gamma, d_x, d_y, d_z\right) = \begin{bmatrix} R_{11} & R_{12} & R_{13} & d_x \\ R_{21} & R_{22} & R_{23} & d_y \\ R_{31} & R_{32} & R_{33} & d_z \\ 0 & 0 & 0 & 1 \end{bmatrix}, \tag{3}$$

where α, β and γ represent the rotation angles about *x*, *y*, and *z*- axis and the d_x, d_y and d_z are translation components along the same axes. Expanding R_{ij} one yields a trigonometric relations based on the angles α, β and γ (Horn 1984). The challenging aspect of T_a^b evaluation is that the solution is highly non-linear. There are number of algorithms to evaluate the homogeneous transformation matrices from cloud of points, proposed in literature since 1980s (Besl and McKay 1992; Brou 1984), which, most typically, aim to minimize the sum of squared errors (SSE):

$$SSE = \sum_{i}^{n} \| T_a^b \boldsymbol{p_{a,i}} - \boldsymbol{p_{b,i}} \|^2 \tag{4}$$

Likewise, TCP of cobot can be assumed as rigid body that moves within the three different frames of references that are the Laser Tracker (LT), the machine vision system based on the OptiTrack cameras frame (MVS) and robot frame (RDK).

The cobot and virtual environment (RoboDK-RDK) reference frames are coincident and centered in the cobot base, with the z-axis coincident with the "shoulder-S" axis of the cobot, as shown in Fig. 6a. The Tool Center Point (TCP) is a virtual point; therefore, it cannot be directly measured by the machine vision system and the laser tracker. In fact, the LT measures the SMR hold at the center of the gripper, while the MVS acquires the location of passive reflectors on the surface of gripper. To evaluate the positioning error of cobot, it is important to bring, i.e. to register, the coordinate frames of the machine vision cameras, of the laser tracker, and of the cobot frame to a global coordinate frame (GL) which can be arbitrarily defined.

Figure 6a represents coordinate frames of the cameras (MVS), laser tracker (LT) and robot (RDK) as frame with all the corresponding transformation matrixes. Spatial coordinates of MVS, RDK and LT system necessitate the transformation into

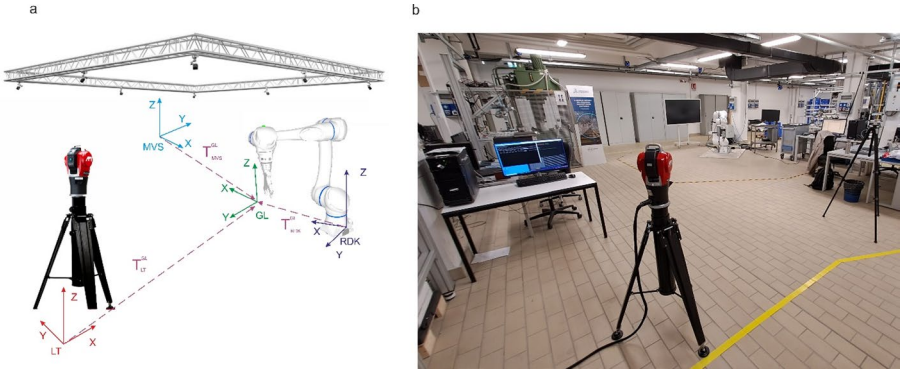

Fig. 6 **a** Homogeneous transformation evaluation in virtual environment **b** Real experimental area

GL coordinate frame to be consistent in the position and orientation measurements. The coordinate transformation of the tool center point (TCP) positions is performed based on homogeneous transformation matrix consisting of rotation and translation transformation components. However, fixing the global frame on a stationary object or frame resulted in additional challenges i.e. difficulty with orientation, mismatches of points due to different methods of data acquisition. Therefore, a three-point registration method was resorted to (Karl and Wyk 2016). The method consists of creating the reference frame based on linear movement of the TCP along 3 vectors representing x_{GL}, y_{GL} and z_{GL} axis that was further used as global reference coordinate frame. The movement of cobot was constrained by vector length of 100 mm in three orthogonal directions. The rigid-body movement of the gripper along the prescribed line with SMR and markers ensure that lines created in corresponding coordinate frames remain parallel and degrades the issue related to the evaluation of orientation of the frames.

To bring the coordinate frames of laser tracker (LT), machine vision system (MVS) and RoboDK frame (RDK) into global frame (GL) of reference, transformation matrices T_{LT}^{GL}, T_{MVS}^{GL} and T_{RDK}^{GL} are estimated. Transformation matrices for all three coordinate frames are evaluated moving TCP onto $p_{x,y,z,i}$ points illustrated in Fig. 7. In total, 12 points have been measured with 10 replications per point according to the 1st step of the experimental procedure described in Sect. 2.1. After the registration, the position errors can be written as:

$$\boldsymbol{e_{LT,GL}} = T_{LT}^{GL}\boldsymbol{p_{LT}} - \boldsymbol{p_{GL}} \tag{5}$$

$$\boldsymbol{e_{MVS,GL}} = T_{MVS}^{GL}\boldsymbol{p_{MVS}} - \boldsymbol{p_{GL}} \tag{6}$$

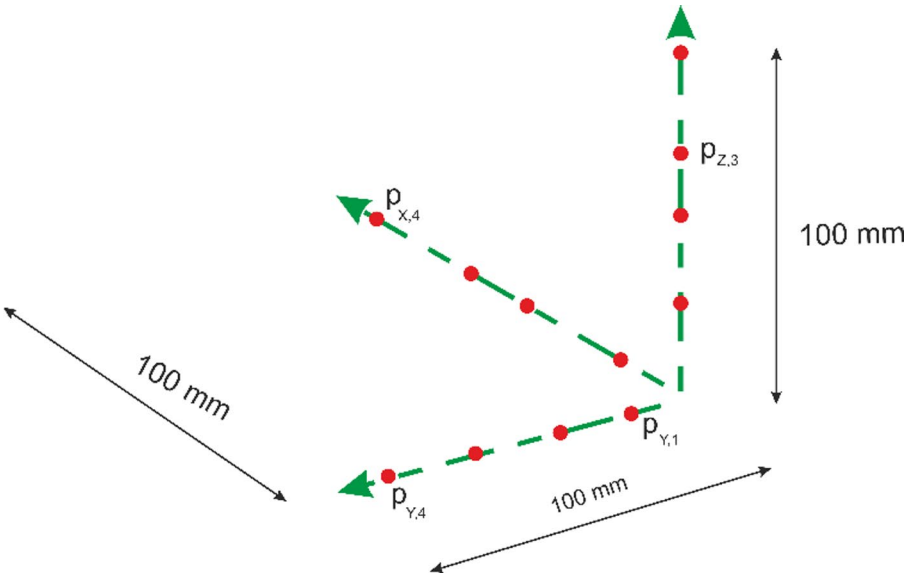

Fig. 7 Evaluation of the Transformation matrices with p representing the points

$$\boldsymbol{e_{RDK,GL}} = T_{RDK}^{GL}\boldsymbol{p_{RDK}} - \boldsymbol{p_{GL}}, \tag{7}$$

where, $\boldsymbol{p_{LT}}, \boldsymbol{p_{RDK}}, \boldsymbol{p_{MVS}}$ and $\boldsymbol{p_{GL}}$ are the points in corresponding frame of references. These errors $\boldsymbol{e}$ are the residuals of the registration, and their average and standard deviation represent the accuracy and reproducibility uncertainty contribution due to the registration.

2.4 GPR based error prediction and detection system.

After the evaluation of homogeneous transformation matrices per each coordinate frame, the experimental plan to estimate positioning error in the working area can be performed, and relying on the calibrated registration matrixes measured data can be expressed in the same global coordinate frame GL. Homogeneous transformation of spatial coordinates into GL coordinates enables to evaluate the positioning errors in LT and MVS coordinates with respect to cobot coordinate system RDK. To apply the GPR modelling to the case in hand, the training of the model is done on the 2nd phase of the experimental procedure, i.e. on the DOE points. Specifically, robot axes can be calibrated with respect to the two exteroceptive sensors system: the laser tracker, thus enabling the evaluation of the positioning error $\boldsymbol{e_{LT,DOE}}$, and the OptiTrack, associated with the error $\boldsymbol{e_{MVS,DOE}}$, as:

$$\boldsymbol{e_{LT,DOE}} = T_{RDK}^{GL}\boldsymbol{p_{RDK}} - T_{LT}^{GL}\boldsymbol{p_{LT}} \tag{8}$$

$$\boldsymbol{e_{MVS,DOE}} = T_{RDK}^{GL}\boldsymbol{p_{RDK}} - T_{MVS}^{GL}\boldsymbol{p_{MVS}}, \tag{9}$$

where $T_{RDK}^{GL}\boldsymbol{p_{RDK}}$, $T_{LT}^{GL}\boldsymbol{p_{LT}}$ and $T_{MVS}^{GL}\boldsymbol{p_{MVS}}$ are the points (collected in the second experimental phase) in the local coordinate frames RDK, LT and MVS that are transformed into global frame of reference. Furthermore, to improve metrological performances of the machine vision system, it can be calibrated with respect to the laser tracker by evaluating $\boldsymbol{e_{MVS-LT}}$ as in Eq. (10) obtained by combining Eq. (8) and Eq. (9):

$$\boldsymbol{e_{MVS-LT,DOE}} = T_{MVS}^{GL}\boldsymbol{p_{MVS}} - T_{LT}^{GL}\boldsymbol{p_{LT}} = \boldsymbol{e_{LT,DOE}} - \boldsymbol{e_{MVS,DOE}} \tag{10}$$

Once errors have been estimated, prediction models can be trained by feeding $\boldsymbol{e_{LT,DOE}}$ and $\boldsymbol{e_{LT,DOE}} - \boldsymbol{e_{MVS,DOE}}$ into the GPR model as responses and using 3D spatial coordinates $\boldsymbol{TCP}$ and the speed of the cobot v as regressors. Once the GPR models with $\widehat{\boldsymbol{e_{MVS-LT}}(\boldsymbol{TCP}, v)}$ and $\widehat{\boldsymbol{e_{LT}}(\boldsymbol{TCP}, v)}$ are trained, the DT system validation is performed on new points according to the 3rd phase of the experimental procedure. Results of validation in terms of RMSE, i.e. the standard deviation, and average of the residuals well describe the physical to virtual (P2V) surrogate modelling uncertainty contribution due to reproducibility and accuracy. Finally, let indicate residuals of the GPR surrogate model as $\boldsymbol{r_{LT}} = \boldsymbol{e_{LT}} - \widehat{\boldsymbol{e_{LT}}}$ and $\boldsymbol{r_{MVS-LT}} = \boldsymbol{e_{MVS-LT}} - \widehat{\boldsymbol{e_{MVS-LT}}}$.

GPR model training can be computationally demanding for big datasets. But, with the available dataset that accounts for around 558 positions, GPR model was derived in MATLAB 2022b running on Windows 11 operating system with 64 GB of RAM within 20 min.

2.5 Metrological characterization of performance

To begin with, a characterization of the system as is has been performed. Accordingly, accuracy and precision of the cobot axes positioning can be evaluated as the average and the standard deviation of errors in the operative range, i.e. $\overline{\boldsymbol{e}_{\boldsymbol{DOE}}}$ and $\boldsymbol{s}\left(\boldsymbol{e}_{\boldsymbol{DOE}}\right)$.

Once the DT correction and control system has been established, metrological characterization shall be performed to robustly and traceably assess performances, and to take decisions, e.g. path planning or maintenance, within a metrological framework. As reported in the workflow of Fig. 3, path prediction is performed based on the cobot axes calibration and surrogate model training performed on the laser tracker data. Propagation of uncertainty is performed according to the law of uncertainty propagation (LUP) (JCGM 100:2008) and estimating and propagating the different metrological characteristics, i.e. accuracy, resolution, reproducibility, of the influencing factors.

The first, the estimation of the uncertainty of the bias-corrected positioning of the cobot can be carried out. According to Sect. 2, the corrected position can be written as $\boldsymbol{TCP_c} = \boldsymbol{TCP} - \widehat{\boldsymbol{e_{LT}}}$. Metrological models can be written to cater for the metrological characteristics of the variables, resulting in the standard uncertainty:

$$\boldsymbol{u}\left(\boldsymbol{TCP_c}\right) = \sqrt{\boldsymbol{reprod}_{TCP}^2 + \frac{\boldsymbol{resol}_{TCP}^2}{3} + \boldsymbol{s}^2\left(\boldsymbol{e}_{\boldsymbol{LT,GL}}\right) + \frac{\overline{\boldsymbol{e}_{\boldsymbol{LT,GL}}}^2}{3} + \boldsymbol{u}_{LT}^2 + \boldsymbol{s}^2\left(\boldsymbol{r}_{\boldsymbol{LT}}\right) + \frac{\overline{\boldsymbol{r}_{\boldsymbol{LT}}}^2}{3}} \quad (11)$$

$$\boldsymbol{reprod}_{TCP}^2 = \frac{\sum_{i=1}^{n} \boldsymbol{s}^2\left(\boldsymbol{e}_{\boldsymbol{LT,GL};i}\right)}{n} \quad (12)$$

$$\boldsymbol{u}\left(\widehat{\boldsymbol{e_{LT}}}\right) = \sqrt{\boldsymbol{s}^2\left(\boldsymbol{e}_{\boldsymbol{LT,GL}}\right) + \frac{\overline{\boldsymbol{e}_{\boldsymbol{LT,GL}}}^2}{3} + \boldsymbol{u}_{LT}^2 + \boldsymbol{s}^2\left(\boldsymbol{r}_{\boldsymbol{LT}}\right) + \frac{\overline{\boldsymbol{r}_{\boldsymbol{LT}}}^2}{3}} \quad (13)$$

Specifically, the TCP is affected by the reproducibility, $\boldsymbol{reprod}_{TCP}^2$, and the resolution, $\boldsymbol{resol}_{TCP}$, of the angular encoders and the collaborative robot motors. These can respectively be evaluated as the variance of replicated positionings at different n locations, see Eq. (12), and as the equivalent variance associated with a uniform distribution having range of variability equal to the encoder resolution. The bias estimate correction, $\widehat{\boldsymbol{e_{LT}}}$, results from the registration of traceable laser tracker measurements to the GL coordinate frame. Accordingly, when correcting the bias, the uncertainty $\boldsymbol{u}\left(\widehat{\boldsymbol{e_{LT}}}\right)$ of such correction term shall include several contributions pertaining to registration residual errors $\boldsymbol{e}_{\boldsymbol{LT,GL}}$, traceability of the laser tracker and model residuals $\boldsymbol{r}_{\boldsymbol{LT}}$. In particular, the precision and accuracy of the surrogate model prediction can be evaluated, respectively, as the variance, $\boldsymbol{s}^2\left(\boldsymbol{r}_{\boldsymbol{LT}}\right)$, and the average, $\overline{\boldsymbol{r}_{\boldsymbol{LT,GL}}}$, of the GPR residuals, $\boldsymbol{r}_{\boldsymbol{LT}}$. The error of registration of the coordinate

frames, i.e. from LT to GL, is estimated considering the variance, $s^2\left(e_{LT,GL}\right)$, and the average, $\overline{e_{LT,GL}}$, of the registration error, $e_{LT,GL}$. In both cases, reproducibility and accuracy can be associated with a normal and uniform distribution to allow variance evaluation. Last, laser tracker traceability, u_{LT}^2, can be evaluated from the calibration standard uncertainty 10 µm+0.02·L µm/m (where L is the measurement length expressed in meters).

Furthermore, to assess whether residual errors after the bias correction control (that can be detected by the MVS), i.e. $\widehat{e_{LT}} - e_{MVS}$, are within expected, i.e. predicted, values $e_{\widehat{MVS-LT}}$, $\widehat{e_{LT}} - e_{MVS}$ can be compared with the prediction $e_{\widehat{MVS-LT}}$. Such comparison shall be performed by a hypothesis test based on the Student-t distribution which requires to evaluate standard uncertainties by combining relevant influence factors:

$$u\left(\widehat{e_{LT}} - e_{MVS}\right) = \sqrt{u^2\left(\widehat{e_{LT}}\right) + reprod_{MVS}^2 + \frac{resol_{MVS}^2}{3} + s^2\left(e_{MVS,GL}\right) + \frac{\overline{e_{MVS,GL}}^2}{3}} \quad (14)$$

$$u\left(e_{MVS}\right) = \sqrt{reprod_{MVS}^2 + \frac{resol_{MVS}^2}{3} + s^2\left(e_{MVS,GL}\right) + \frac{\overline{e_{MVS,GL}}^2}{3}} \quad (15)$$

$$\begin{aligned} u\left(e_{\widehat{MVS-LT}}\right) \\ = \sqrt{\begin{array}{l} s^2\left(e_{LT,GL}\right) + \frac{\overline{e_{LT,GL}}^2}{3} + s^2\left(e_{MVS,GL}\right) + \frac{\overline{e_{MVS,GL}}^2}{3} \\ \quad + s^2\left(r_{MVS-LT}\right) + \frac{\overline{r_{MVS-LT}}^2}{3} + reprod_{MVS}^2 + \frac{resol_{MVS}^2}{3} + u_{LT}^2 \end{array}} \end{aligned} \quad (16)$$

$$t_{\exp} = \frac{\left(\widehat{e_{LT}} - e_{MVS}\right) - e_{\widehat{MVS-LT}}}{\sqrt{u^2\left(\widehat{e_{LT}} - e_{MVS}\right) + u^2\left(e_{\widehat{MVS-LT}}\right)}} \quad (17)$$

Specifically, the t statistics, see Eq. (17), requires evaluating the uncertainty of the residual errors after the bias correction control, $u\left(\widehat{e_{LT}} - e_{MVS}\right)$, and of the predicted measurement error of the MVS with respect to the LT, $u\left(e_{\widehat{MVS-LT}}\right)$. In particular, Eq. (14) combines the uncertainty of the correction as estimated by the LT, i.e. $u^2\left(\widehat{e_{LT}}\right)$ as detailed in Eq. (13), and the uncertainty of the MVS detailed in Eq. (15), which combines the reproducibility, $reprod_{MVS}^2$ computed as in Eq. (12), and the resolution, $resol_{MVS}$, of the MVS, and the variance, $s^2\left(e_{MVS,GL}\right)$, and average, $\overline{e_{MVS,GL}}$, of the registration error $e_{MVS,GL}$ of the MVS coordinate frame to the global coordinate frame. Similarly, the standard uncertainty of the predicted error between the MVS and the LT of Eq. (17) combines relevant contributions previously detailed and the model residuals variance, $s^2\left(r_{MVS-LT}\right)$, and average, $\overline{r_{MVS-LT}}$.

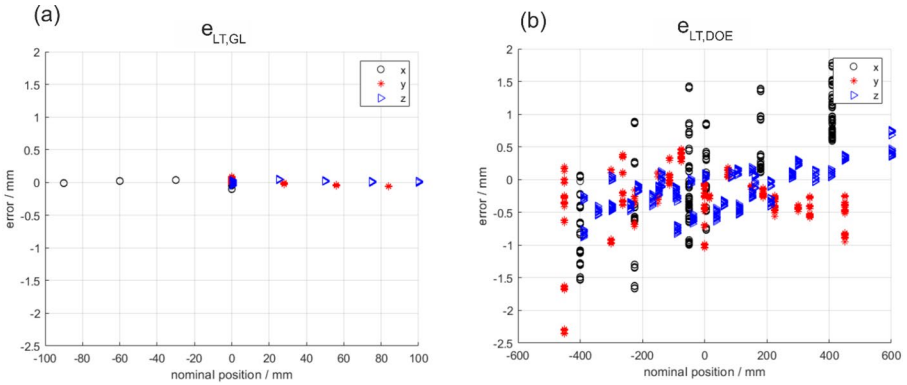

Fig. 8 Transformation error **a** transformation error for LT **b** error measurement of 2nd phase points of DOE of LT

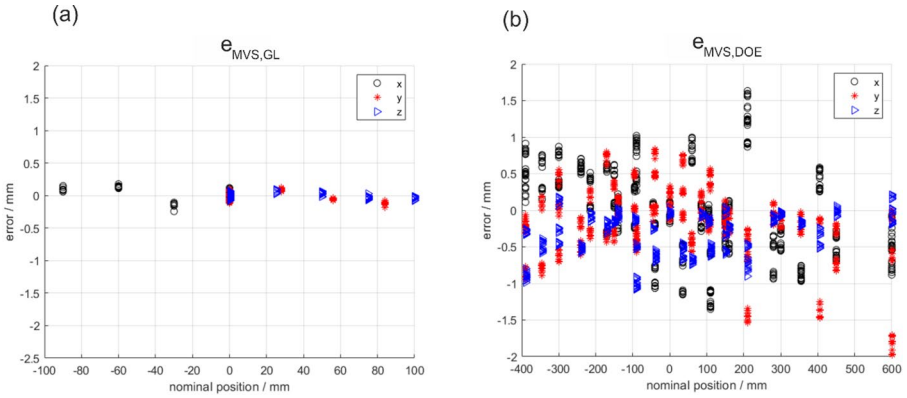

Fig. 9 Cobot positioning error with respect to camera system **a** homogeneous transformation errors of the camera **b** error measurement of 2nd phase points of DOE of MVS

3 Result and discussions

3.1 Evaluation of homogeneous transformation error and position error measurement

First, the homogeneous transformation matrixes to enable coordinate transformations are evaluated by means of the three-point registration method described in Sect. 2.3. Residuals of the registration matrix estimation are shown in Figs. 8, 9, 10a and present a distribution not significantly different from a normal distribution with a confidence level of 95% according to Anderson–Darling test. Average and standard deviations are reported in Table 2, which allow evaluating the contribution of accuracy and reproducibility to measurement uncertainty due to the registration, as detailed in Sect. 2.5. Furthermore, replicated positioning allows to evaluate the reproducibility of each measuring system, i.e. the angular encoders and the MVS, which respectively

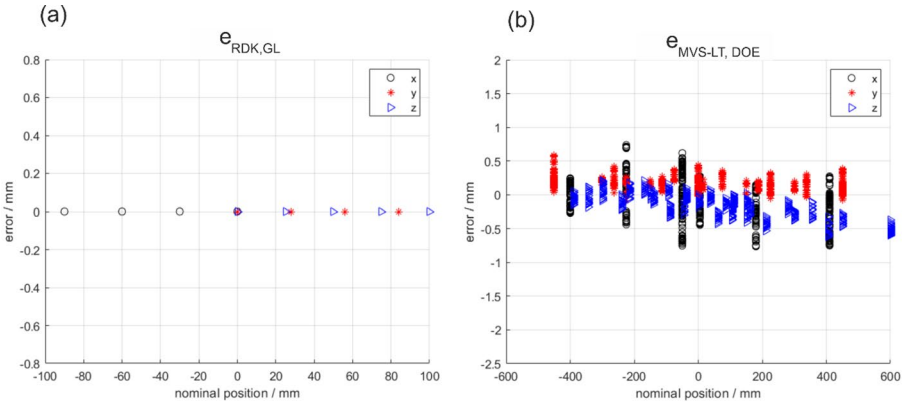

Fig. 10 RoboDK and Camera error **a** RDK transformation error with respect to GL frame **b** Camera error with respect to the LT

Table 2 Average and standard deviation of residuals error of rototranslation

	x		y		z	
	$\overline{e}$/mm	$s\,(e)$/mm	$\overline{e}$/mm	$s\,(e)$/mm	$\overline{e}$/mm	$s\,(e)$/mm
$e_{LT,GL}$	0.000	0.046	0.000	0.042	0.000	0.032
$e_{MVS,GL}$	0.000	0.080	0.000	0.070	0.000	0.042

These contribute to accuracy and reproducibility of the registration operation. The zero value of the average is consistent with the theoretical residual distribution

Table 3 Performance of the system as is. Notice the poor performances in terms of accuracy and precision

	x		y		z	
	$\overline{e}$/mm	$s\,(e)$/mm	$\overline{e}$/mm	$s\,(e)$/mm	$\overline{e}$/mm	$s\,(e)$/mm
$e_{LT,DOE}$	0.073	0.816	−0.333	0.479	−0.171	0.331
$e_{MVS,DOE}$	0.000	0.628	−0.159	0.479	−0.332	0.288
$e_{MVS-LT,DOE}$	−0.074	0.324	0.174	0.107	−0.161	0.182

results in $\boldsymbol{reprod}_{\boldsymbol{TCP}} = \{0.0037, 0.0059, 0.0072\}$ mm and $\boldsymbol{reprod}_{\boldsymbol{MVS}} = \{0.023, 0.019, 0.028\}$ mm.

Once the transformation matrixes are estimated, they can be applied to evaluate the raw position errors needed to train the GPR surrogate model. The investigation of such errors is relevant because it describes the state of the system as is, i.e. before any correction and control strategy based on the DT is deployed. Table 3 reports the mean and standard deviation of the errors prior any bias correction and control strategies are implemented; scatter plot of the errors is reported in Figs. 8, 9 and 10b.

Additionally, relying on the experimental plan, main effects and interaction plots can be analyzed to qualitatively estimate the effect of the considered influence factors on the positioning accuracy (as it will be shown in the next Figs. 11 and 12). The laser tracker measured errors (enabling the calibration of the cobot axes) allows appreciating a systematic trend in the TCP position on the z-axis that is illustrated in Fig. 8b. While LT-measured positioning errors robustly show constructional and

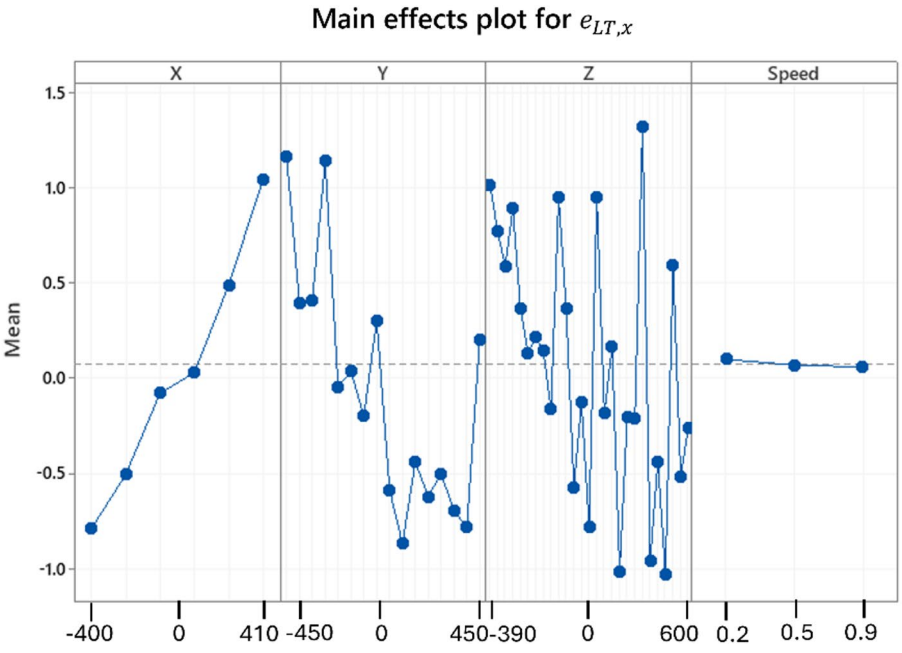

Fig. 11 Main effects plot for the response $e_{LT,X}$ considering four factors that are three spatial coordinates (X, Y, Z) and speed of the cobot

kinematics positioning errors of the robot, the MVS-measured errors shown in the Fig. 9b are also influenced by lower accuracy of sensor and possible systematic errors in the machine vision system. These result in a lack of clear trends in any axis with only slight qualitatively quadratic deviation in the *y-axis* as shown in Fig. 9b. Spatial calibration of the MVS based on the laser tracker can be at last evaluated as reported in Fig. 10b, which shows qualitatively only constant systematic errors to be present as a function of the distance.

The positioning errors e_{LT}, e_{MVS} and e_{MVS-LT} illustrated in Figs. 8, 9 and 10b in the GL coordinate reference system can be mainly ascribed to structural parameter errors due to joint angle deviations, gear transmission error, serial-kinematic link errors and torsional rotation errors (Song et al. 2022). To analyze the main effects and validate qualitative observations from Fig. 8, 9 and 10, Generalized Linear Model (GLM) analysis of $\boldsymbol{e_{LT}}$ is done per each axis considering the three spatial coordinates of the DOE points and the speed (as defined in Sect. 2.2), with 2nd order interactions. GLM is performed in commercial software MINITAB. To highlight systematic effects, only errors measured with LT are considered to dispense with other possible disturbances that might be superposed by less accurate instruments.

Main effect plot reported in Fig. 11 further validates the systematic effect of the nominal coordinates *x, y,* and *z-axis* qualitatively appreciated in the scatter plot; conversely, small effect of speed can be seen for $e_{LT,\mathrm{X}}$. Quantitatively, the GLM model of $e_{LT,\mathrm{X}}$ and $e_{LT,Y}$ show a systematic effect for all the motion axes and the speed with *p*-value smaller than 0.05 However, the effect of Y coordinate was not significant for $e_{LT,Z}$ with p-value = 0.739 while the speed, *X* and *Z* coordinates effect were

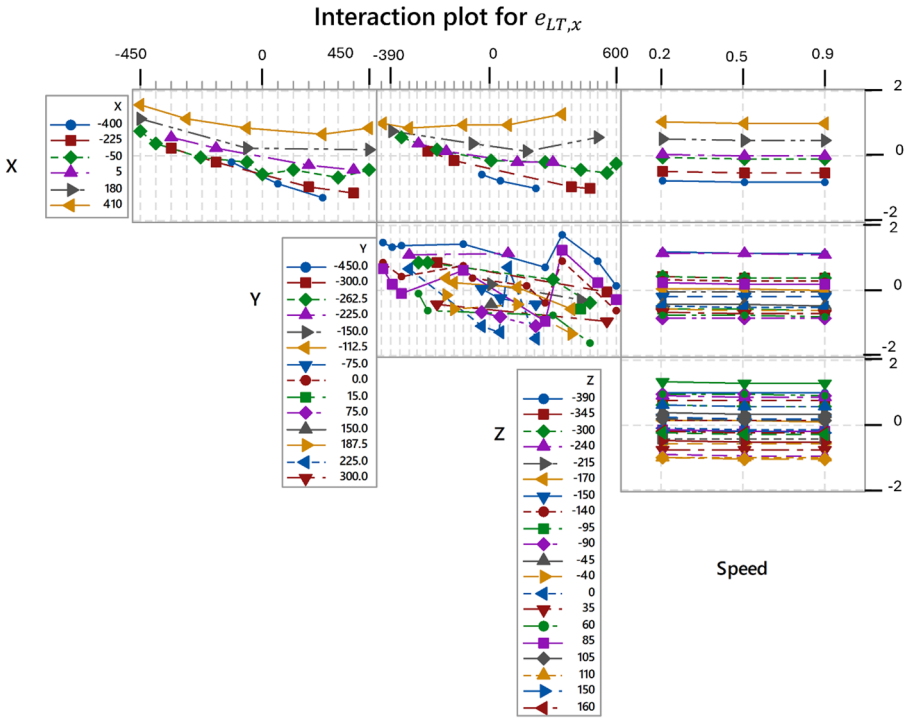

Fig. 12 Interaction plot of coordinates X, Y, Z and speed for the response $e_{LT,X}$

significant with *p*-value smaller than 0.05. To analyse the combined effect of input factors the interaction plot has been performed and it is shown only for $e_{LT,X}$ in Fig. 12. The interaction plot shows that there is no interaction between the speed and spatial coordinates *X, Y* and *Z*. However, the combined effect of *Y- Z, X–Y* and *X–Z* coordinates is present due to the non-orthogonal and coupled motion of cobot axes.

3.2 Training of GPR surrogate model

The experimentally observed input dataset for modeling GPR consists of four coordinates namely three nominal coordinates X, Y, Z in RDK frame and the speed of the robot. A Bayesian approach was used to select the GPR model parameter, i.e. the kernel function and the regression function (Maculotti et al. 2023). An Automatic Relevance Determination Squared Exponential (ARDSE) kernel with a constant regression function was selected (Leco et al. 2022; Leco and Kadirkamanathan 2021). In these models, the parameters that have the higher weights will have a bigger impact on the model. For sake of brevity, GPR training results for $e_{LT,X}$ and $e_{MVS-LT,X}$ prediction is visualized in Figs. 13 and 14, respectively; results related to other coordinate axes are reported in the Annex.

Qualitative analysis of true response to predicted response shows a good linearity in Fig. 13a, and Normal Probability plot (NPP) of residuals, depicted in Fig. 13b, does not show relevant deviations from normality Chi-square test with *p*-value of

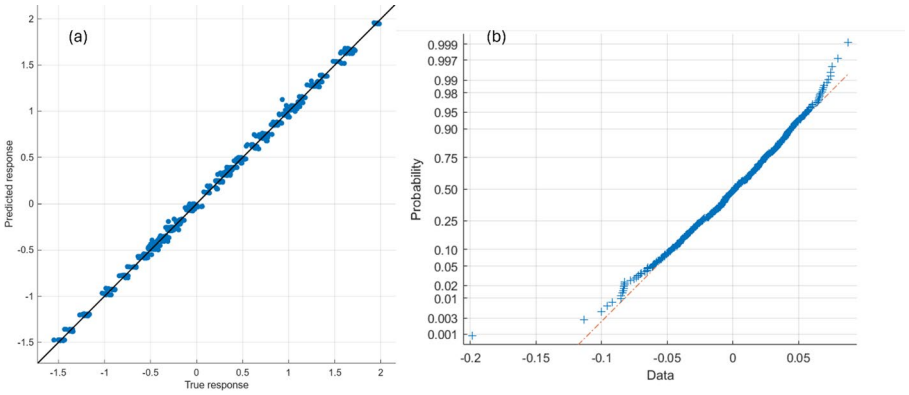

Fig. 13 GPR model for e_{LT} for the X-axis **a** true response and GPR prediction **b** NPP of GPR residuals

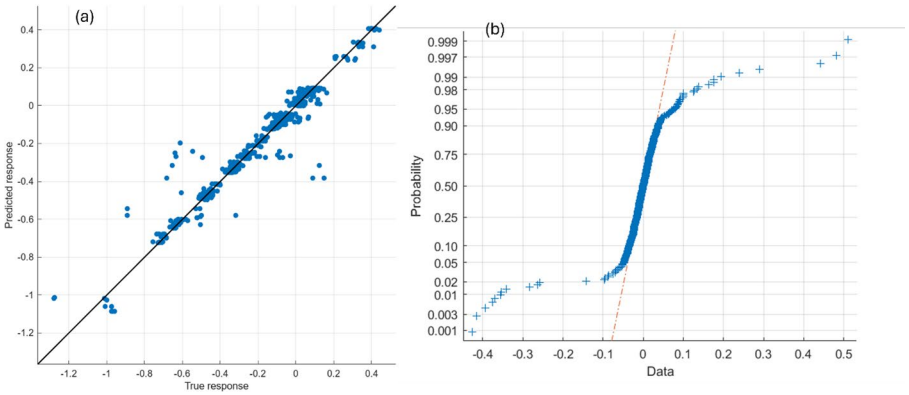

Fig. 14 GPR model for $e_{MOT-LT,X}$ for the X-axis **a** true response and GPR prediction **b** NPP GPR residuals

0.643. The analysis of the predicted and true values for GPR model of $e_{MOT-LT,X}$ shows a larger dispersion (see Fig. 14a), due to the MVS, with a hypernormal trend (see Fig. 14b).

3.3 Uncertainty evaluation of DT system

The metrological characterization and uncertainty evaluation allow establishing traceability for the developed DT. According to the methodology described in Sect. 2.5, the first, the uncertainty of the corrected TCP position is evaluated. This needs propagating, according to Eq. (11), contributions from the positioning reproducibility of the cobot (see Sect. 3.1), the registration contributions (reported in Table 2), the traceability contribution of the laser tracker, i.e. 0.0004 mm, and the accuracy and reproducibility of the surrogate prediction model, which can be estimated from the mean and standard deviation of the residuals $\boldsymbol{r_{LT}}$, as reported in Table 4. Accordingly, the expanded uncertainty of the corrected position $\boldsymbol{U}\,(\boldsymbol{TCP_c})$, evaluated at

Table 4 Average and standard deviation of residuals error of surrogate GPR systematic error modelling

	x		y		z	
	$\overline{e}$/mm	$s\,(e)$/mm	$\overline{e}$/mm	$s\,(e)$/mm	$\overline{e}$/mm	$s\,(e)$/mm
r_{LT}	0.000	0.037	0.000	0.034	0.000	0.079
r_{MVS-LT}	0.000	0.069	0.000	0.061	0.000	0.093

These describe the accuracy (negligible) and reproducibility of the systematic error correction

a confidence level of 95%, is reported in Eq. (18), and has as main contribution the prediction uncertainty of the GRP model $\boldsymbol{u}\,(\widehat{\boldsymbol{e_{LT}}})$:

$$\boldsymbol{U}\,(\boldsymbol{TCP_c}) = \{0.118, 0.109, 0.171\}\ \text{mm} \tag{18}$$

$$\boldsymbol{U}\,(\widehat{\boldsymbol{e_{LT}}}) = \{0.117, 0.108, 0.170\}\ \text{mm} \tag{19}$$

Next, the evaluation of the uncertainty to allow real-time identification of positioning error, despite the systematic correction, can be carried out. This requires evaluating the $\boldsymbol{u}\,(\widehat{\boldsymbol{e_{LT}}} - \boldsymbol{e_{MVS}})$., i.e. the uncertainty of the MVS measurements with respect to corrections, and the predicted error based on the MVS, i.e. $\boldsymbol{u}\left(\boldsymbol{e}_{\widehat{\boldsymbol{MVS-LT}}}\right)$. The former, as per Eq. (14) and Eq. (15) propagates the contribution from the error prediction based on the LT, evaluated in Eq. (18), and the position measurements based on the MVS, i.e. $\boldsymbol{u}\,(\boldsymbol{e_{MVS}})$; the latter is instead evaluated according to Eq. (17). Relevant expanded uncertainty at 95% confidence levels results in:

$$\boldsymbol{U}\,(\widehat{\boldsymbol{e_{LT}}} - \boldsymbol{e_{MVS}}) = \{0.203, 0.182, 0.198\}\ \text{mm} \tag{20}$$

$$\boldsymbol{U}\,(\boldsymbol{e_{MVS}}) = \{0.166, 0.146, 0.102\}\ \text{mm} \tag{21}$$

$$\boldsymbol{U}\left(\boldsymbol{e}_{\widehat{\boldsymbol{MVS-LT}}}\right) = \{0.230, 0.204, 0.214\}\ \text{mm} \tag{22}$$

Significant change in terms of precision is achieved from DT-based prediction, i.e. $\boldsymbol{U}\left(\boldsymbol{e}_{\widehat{\boldsymbol{MVS-LT}}}\right)$, approach compared to MVS measurement for tracking, i.e. $\boldsymbol{U}\,(\boldsymbol{e_{MVS,DOE}})$., that can be seen in the Table 3. Particularly, precision improved from 1.256 mm to 0.230 mm in *x-axis*, from 0.958 mm to 0.204 mm in *y-axis*, and from 0.576 mm to 0.214 mm in *z-axis*, resulting in an average improvement from 0.970 mm to 0.216 mm, i.e. of 77.8%.

The uncertainty in 3D will look like a rectangular envelope in space that is illustrated in Fig. 15 with 200x magnification for test points. Such representation can be useful for path planning in augmented reality or virtual reality, as well as for operator training applications to allow metrological robust and trustworthy deployment of DT.

3.4 Validation of proposed system

Based on the proposed methodology in the Sect. 2.2, the aim of the paper is to correct the positioning error of the cobot and detect the points $\widehat{\boldsymbol{e_{LT}}} - \boldsymbol{e_{MVS}}$ that are bigger than the GPR model of $\boldsymbol{e_{LT}} - \widehat{\boldsymbol{e_{MVS}}}$ in order to proceed with the maintenance. To validate the proposed system, a new set of 36 points randomly chosen on virtual

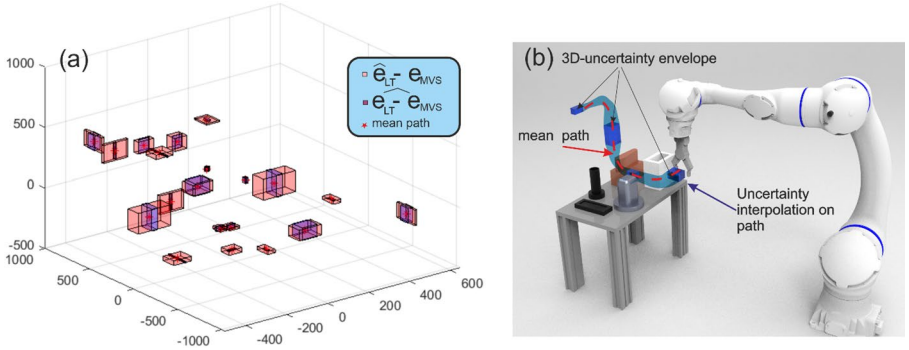

Fig. 15 Illustration of uncertainty of DT system **a** derived 3D-uncertainty of target points magnified for illustration purposes **b** mean interpolation of uncertainty in the path (light blue), 3D-uncertainty envelope on target points of the path (dark-blue boxes)

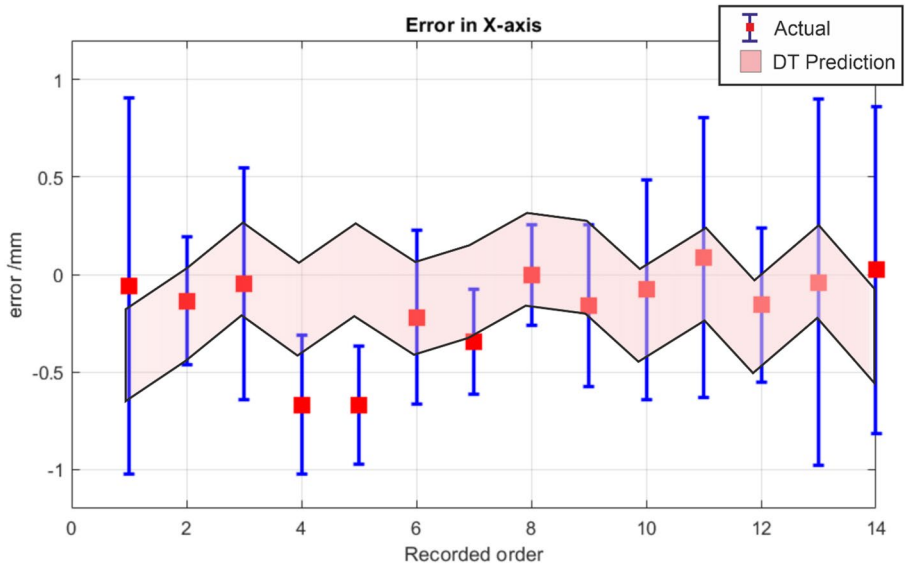

Fig. 16 $e_{LT} - \widehat{e_{MVS}}$ represented as GPR in blue and $\widehat{e_{LT}} - \overline{e_{MVS}}$ as actual evaluation having expanded uncertainty with confidence interval of 95% on the x-axis

space with 10 repetitions are acquired. Based on the GPR training test prediction error for $\widehat{e_{LT}}$, the $\widehat{e_{LT}} - e_{MVS}$ uncertainty is evaluated.

Figures 16, 17 and 18 illustrate the predicted positioning error bands with expanded uncertainty bands for $\widehat{e_{LT}} - e_{MVS}$ depicted as "DT prediction" and the positioning error evaluated from $\widehat{e_{LT}} - \overline{e_{MVS}}$ illustrated as "Actual". The errors are plotted according to the recorded order for the purpose of visualization.

The validation and the comparison of actual and DT-prediction position within a metrological framework, allows to detect unusual positioning errors. In fact, the graphical comparison reported in Figs. 16, 17 and 18 corresponds to a t-test, which

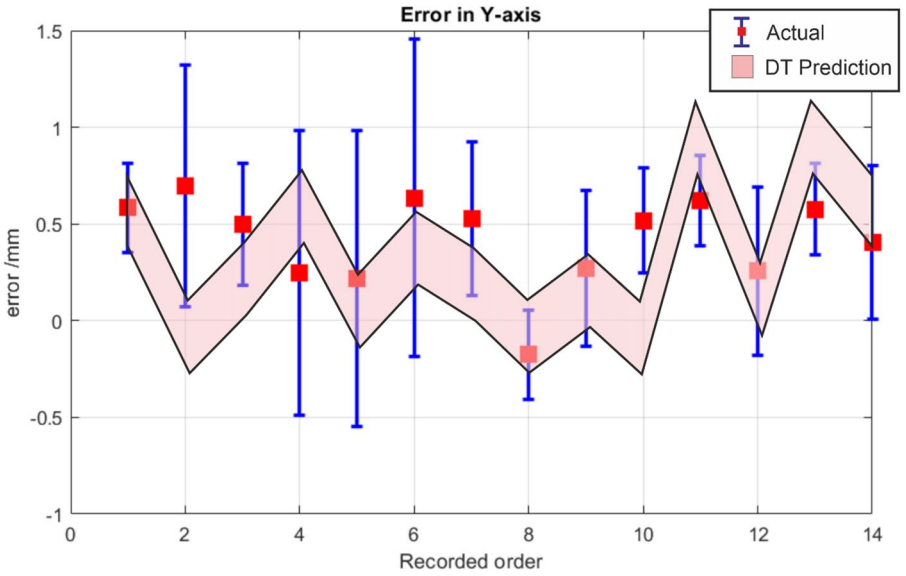

Fig. 17 $e_{LT}\widehat{-e_{MVS}}$ represented as GPR in blue and $\widehat{e_{LT}} - \overline{e_{MVS}}$ as actual evaluation having expanded uncertainty with confidence interval of 95% on the y-axis

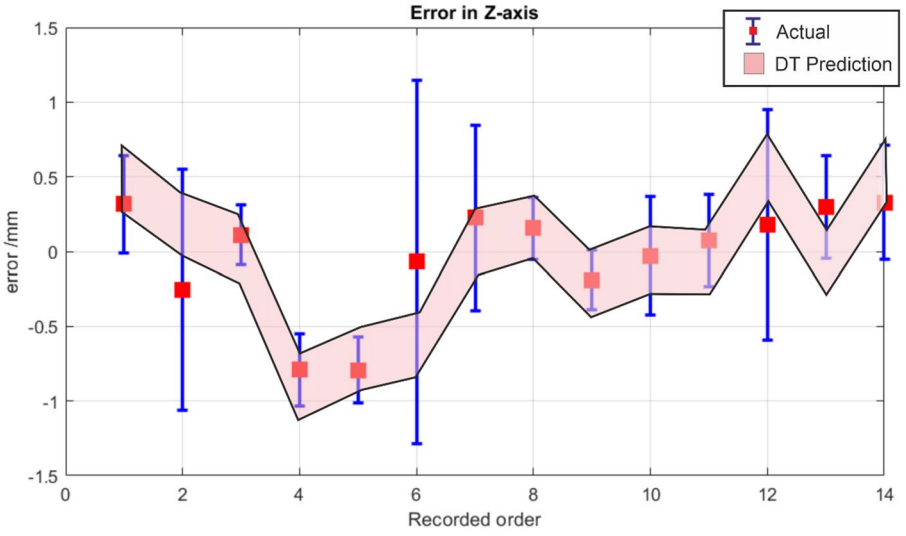

Fig. 18 $e_{LT}\widehat{-e_{MVS}}$ represented as GPR in blue and $\widehat{e_{LT}} - \overline{e_{MVS}}$ as actual evaluation having expanded uncertainty with confidence interval of 95% on the z-axis

by relying on the uncertainty propagation, as per Sect. 2.5, allows to detect anomalies and out of control positioning while catering for the DT control. The evaluation of uncertainty reported in Sect. 3.3 and specifically results shown in Eqs. (19) and (20) elicit such a comparison. This would allow to trigger predictive maintenance of the DT system based on a statistical analysis.

3.5 Discussion

The results showed a significant improvement of the positioning uncertainty of the collaborative robot of 1 order of magnitude, driven by the correction of systematic errors and improved precision. The implemented methodology allows to establish traceability of the DT through the calibration of the error model performed by the laser tracker. This aspect is fundamental to allow a metrological control of the operation of the collaborative robot system, i.e. based on uncertainty propagation and calibration of the error model.

The virtual entity is based on a surrogate error model leveraging a Gaussian Process Regression. The calibration of the motion axes of the robot– instrumental to establish traceability of the error model, is a periodic operation that is regularly performed during maintenance of the system, also in industry. The adoption of a machine learning model, i.e. GPR, allows a scalable implementation approach. In fact, depending on the know-how of the operator, it can be either treated as a black-box model, or as a sophisticated statistical approach.

The availability of the exteroceptive sensors, namely the set of eight infrared cameras, allow real-time update of the error estimation. In particular, statistically significant positioning errors can be metrologically detected– basing on propagated measurement uncertainty—comparing the DT prediction and the cameras measurement, as in Figs. 16, 17 and 18.

When comparing to state-of-the-art approaches, outlined in the literature review of Sect. 1, and summarized in Table 1, the present work exploits a consistent traceable approach, and innovatively propagates the measurement uncertainty of each step in error estimation, correction and coordinate system registration. Although the work leverages state-of-the-art methods (as indicated in Table 1) to calibrate errors, i.e. laser tracker, and to spatially map errors, i.e. a Gaussian Process Regression, the structured design of experiment allows achieving a full correction of the bias (see Table 4) and, despite the propagation of many influence factors in the uncertainty budget, a dispersion of about 0.1 mm– expressed as measurement uncertainty—comparable to some state-of-the-art results, which though only report the error dispersion and do not address a proper uncertainty propagation, which as such are largely underestimated.

In future work, the update of the virtual entity error model will be implemented based on continuous learning from the camera measurements. Conversely, control charts, possibly multivariate, will highlight presence of out-of-control points and drifts of the system, which will deploy ad-hoc recalibration and predictive maintenance of the system. Last, this work demonstrated a methodology considering a limited set of operating conditions. Accordingly, future works will include in the DT surrogate error model the payload, the type of motion, e.g. linear or joint movement,

and include further exteroceptive sensors to monitor the working system and its environment, e.g. accelerometers to measure vibrations of the joints, and temperature sensors. Additional sensors will be instrumental for the application in industrial environment of a metrological DT, and to trace detected out-of-control to most probable error sources. Similarly, future works will leverage more advanced machine vision systems to update the monitoring, and consequently the DT, of the environment to prevent crashes with unexpected obstacles, or presence of operators.

4 Conclusions

The paper proposed a novel method to establish traceability and propagate measurement uncertainty for a Digital Twin of a collaborative robot to correct and detect positioning error. A probabilistic data-driven training based on Gaussian Process Regression is used to predict the positioning errors exploiting a machine vision system and a laser tracker. The metrological characteristics of the DT system are estimated with corresponding uncertainties. The proposed method is demonstrated with the test dataset on an industrial system.

The complexity of HRC system design and particularities of cobot structure introduces several error sources that further propagate into positioning errors. The positioning error is of primary importance in HRC systems as it can lead to serious and unpredictable accidents for humans. The approach allows to estimate the confidence intervals of the positioning of the cobot based on a metrological approach capable of catering for the metrological characteristics and correction of the DT system. The proposed method resulted in an improvement of the positioning precision of about 78% once systematic errors have been corrected. Graphical representation of uncertainty intervals in the 3D space are proposed and are instrumental to allow intuitive training and path planning. In future works, continuous learning from camera measurements will be used to update the virtual entity error model, and the methodology will be extended to cater for wider operating conditions, i.e. payloads, vibration and different types of movements. Also, more advanced machine vision systems will be used to improve environmental monitoring, preventing crashes with obstacles or operators.

Appendix

See Figs. 19, 20, 21, 22, 23, 24, 25 and 26.

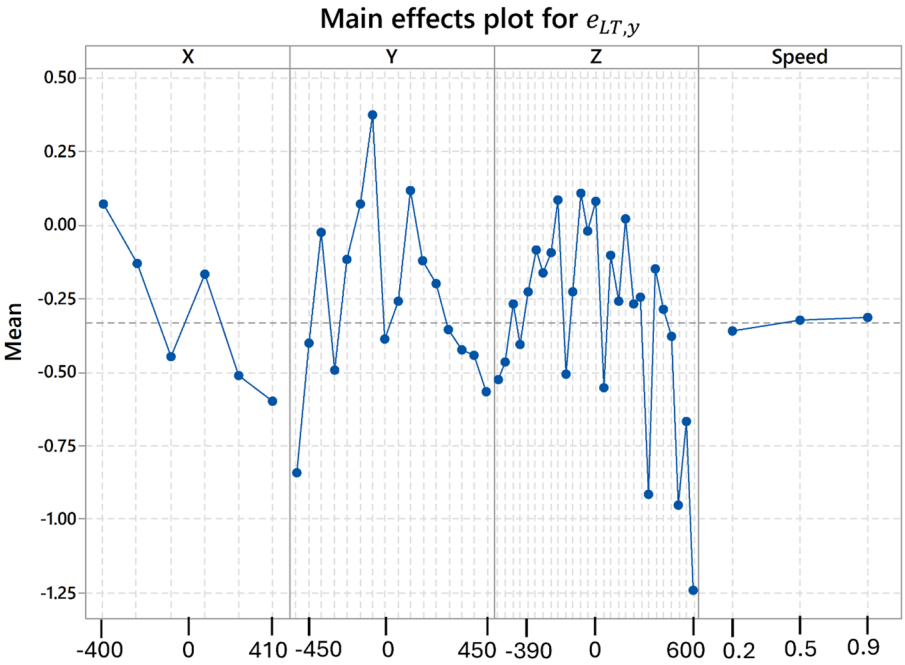

Fig. 19 Main effects plot for the response $e_{LT,y}$ considering four factors that are three spatial coordinates (X, Y, Z) and speed of the cobot

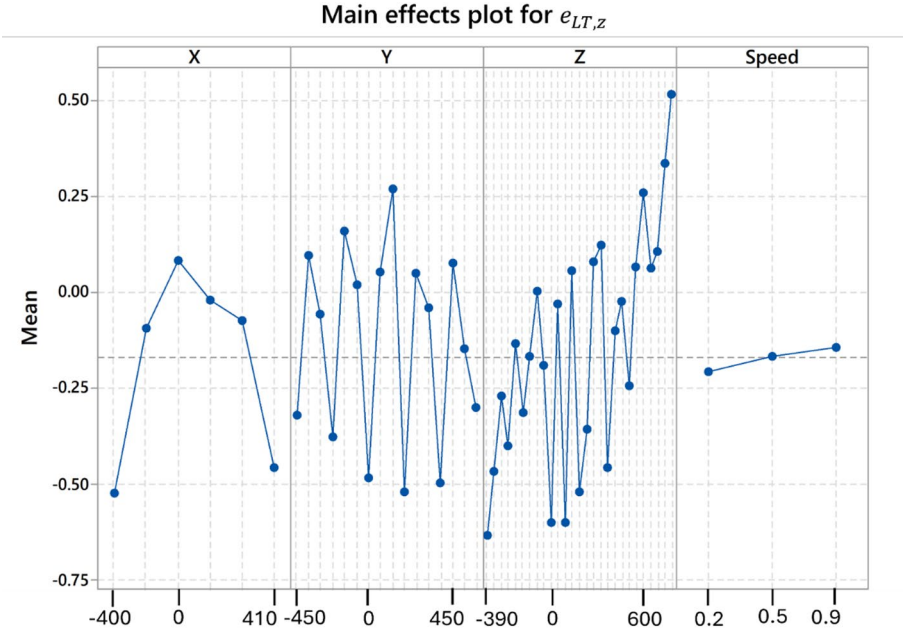

Fig. 20 Main effects plot for the response $e_{LT,z}$ considering four factors that are three spatial coordinates (X, Y, Z) and speed of the cobot

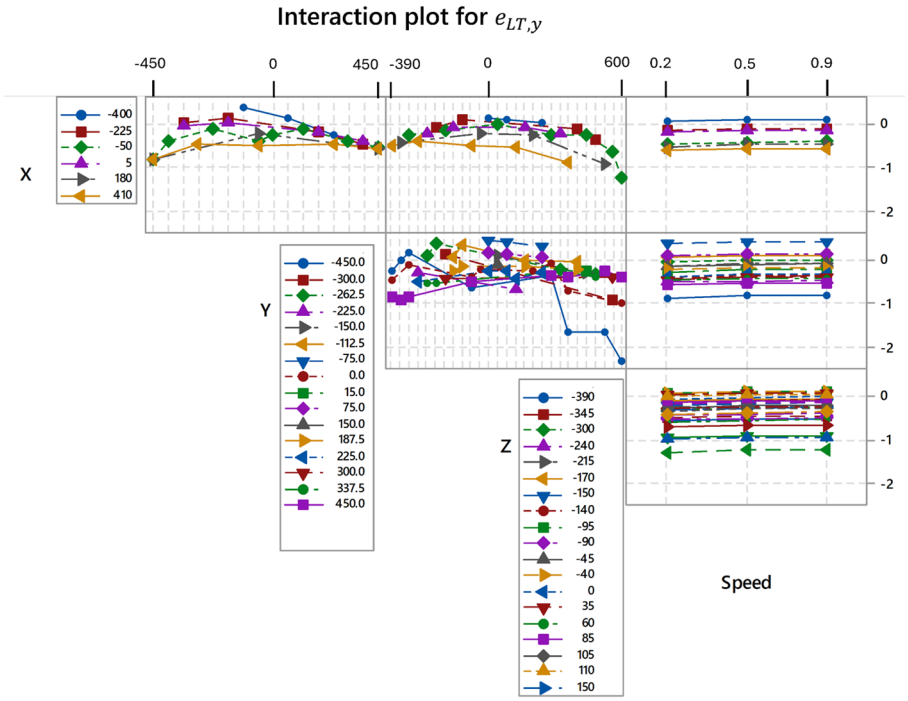

Fig. 21 Interaction plot of coordinates X, Y, Z and speed for the response $e_{LT,y}$

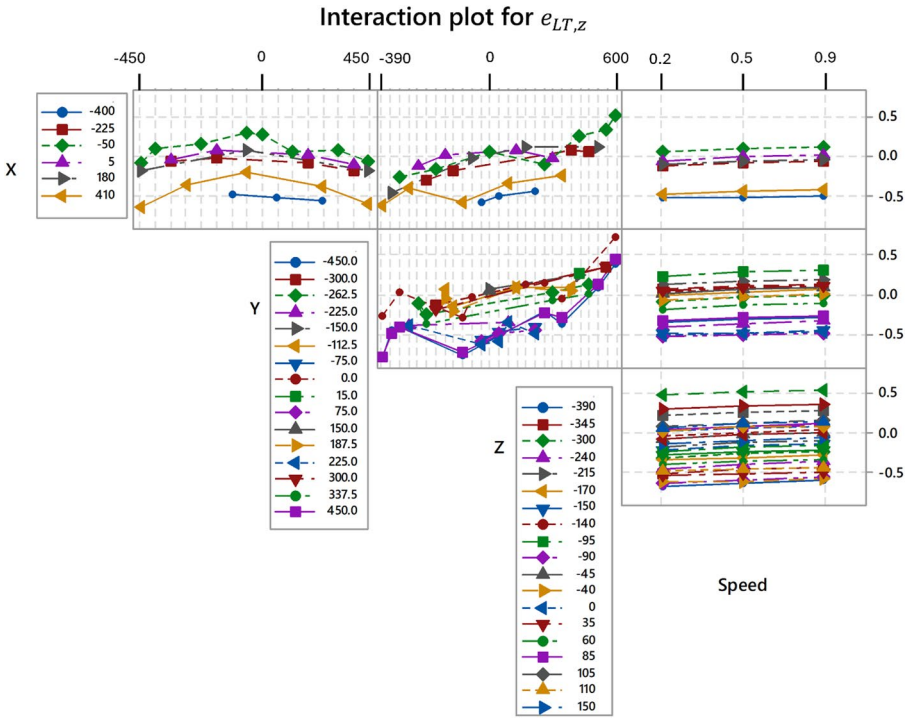

Fig. 22 Interaction plot of coordinates X, Y, Z and speed for the response $e_{LT,z}$

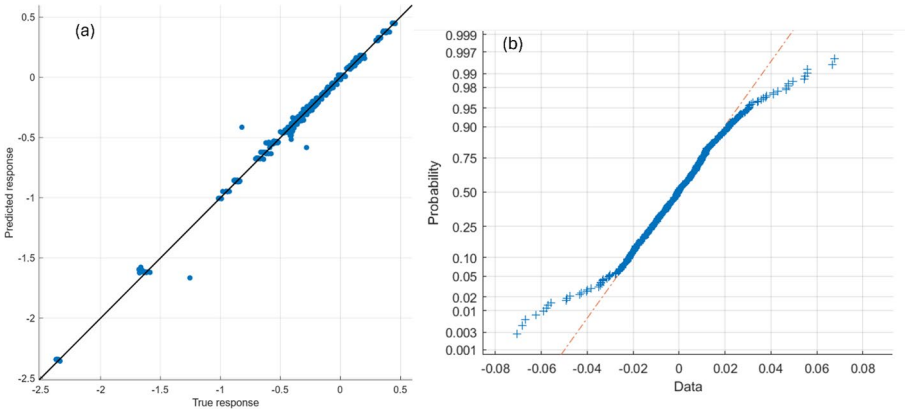

Fig. 23 GPR model for e_{LT} for the Y-axis a) true response and GPR prediction b) NPP of GPR residuals

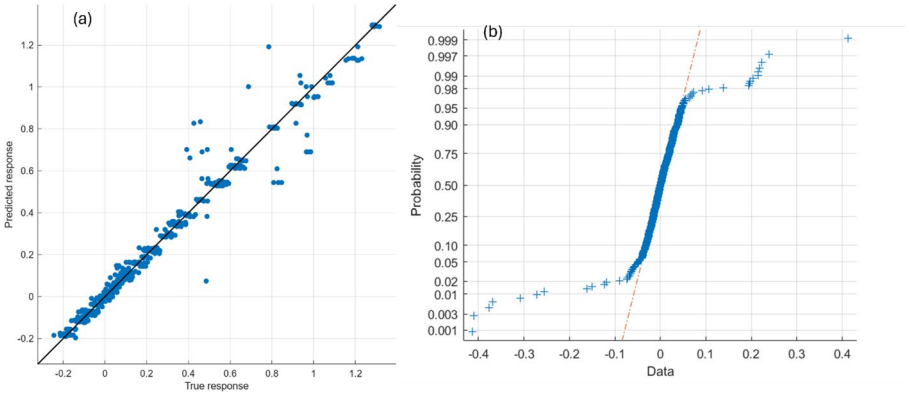

Fig. 24 GPR model for e_{LT} for the Z-axis **a** true response and GPR prediction **b** NPP of GPR residuals

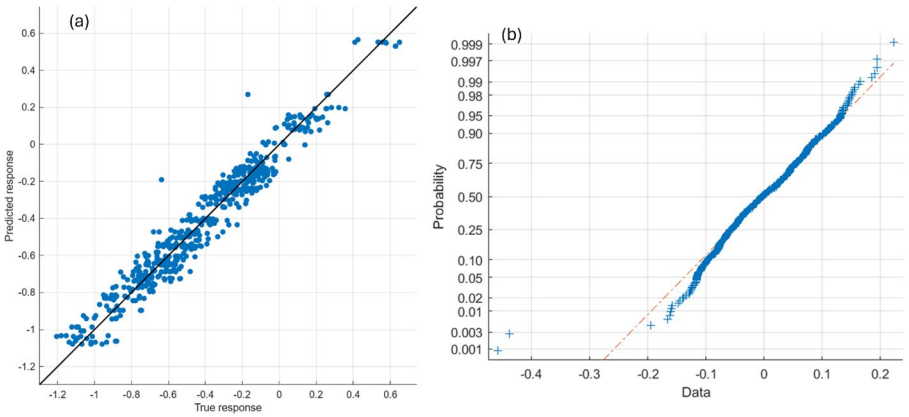

Fig. 25 GPR model for $e_{MOT-LT,Y}$ for the Y-axis **a** true response and GPR prediction **b** NPP GPR residuals

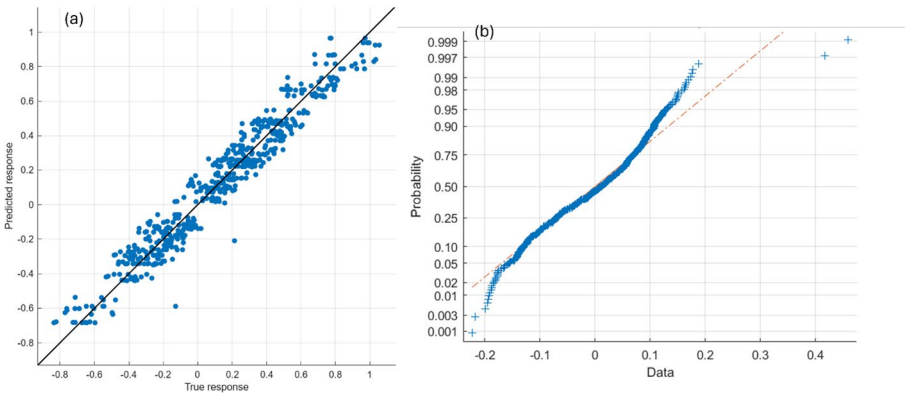

Fig. 26 GPR model for $e_{MOT-LT,Z}$ for the Z-axis **a** true response and GPR prediction **b** NPP GPR residuals

Funding This work has been carried out within the project 23IND08 DI-Vision which has received funding from the European Partnership on Metrology, cofinanced from the European Union's Horizon Europe Research and Innovation Programme and by the Participating States. Views and opinions expressed are however those of the author(s) only and do not necessarily reflect those of the European Union or EURAMET. Neither the European Union nor the granting authority can be held responsible for them.

Data availability Available upon request to the authors.

Declarations

Competing interests The authors have no competing interests to declare that are relevant to the content of this article.

References

Barravecchia F, Bartolomei M, Mastrogiacomo L, Franceschini F (2023a) Redefining human-robot symbiosis: a bio-inspired approach to collaborative assembly. Int J Adv Manufact Technol 128(5):2043–2058. https://doi.org/10.1007/s00170-023-11920-1

Barravecchia F, Mastrogiacomo L, Franceschini F (2023b) A general cost model to assess the implementation of collaborative robots in assembly processes. Int J Adv Manufact Technol 125(11):5247–5266. https://doi.org/10.1007/s00170-023-10942-z

Besl JP and McKay DN (1992) A method for registration of 3-D shapes

Bilal DK, Unel M, Tunc LT, Gonul B (2022) Development of a vision based pose estimation system for robotic machining and improving its accuracy using LSTM neural networks and sparse regression. Robot Comput Integrated Manufact. https://doi.org/10.1016/j.rcim.2021.102262

Bilberg A, Malik AA (2019) Digital twin driven human–robot collaborative assembly. CIRP Ann 68(1):499–502. https://doi.org/10.1016/j.cirp.2019.04.011

Billard AG, Calinon S, Dillmann R (2016) Learning from humans. In: Siciliano B, Khatib O (eds) Springer handbook of robotics. Springer, Berlin, pp 1995–2014. https://doi.org/10.1007/978-3-319-32552-1_74

Brou P (1984) using the gaussian image to find the orientation of objects. Int J Robot Res 3(4):89–125. https://doi.org/10.1177/027836498400300406

Brugali D, Broenink JF, Kroeger T, and Macdonald BA (2014) LNAI 8810 - Simulation, Modeling, and Programming for Autonomous Robots. In Proceedings

Chancharoen R, Chaiprabha K, Wuttisittikulkij L, Asdornwised W, Saadi M, Phanomchoeng G (2022) Digital twin for a collaborative painting robot. Sensors 23(1):17. https://doi.org/10.3390/s23010017

Chen B, Wan J, Shu L, Li P, Mukherjee M, Yin B (2018) Smart factory of industry 4.0: key technologies, application case, and challenges. IEEE Access 6:6505–6519. https://doi.org/10.1109/ACCESS.2017.2783682

Chen X, Zhan Q, Wang Y, and Yao Y (2019) A Comprehensive Positioning Accuracy Compensation Method Based on BP Neural Network of Industrial Robots. In: 2019 4th International Conference on Robotics and Automation Engineering (ICRAE), 24–28. https://doi.org/10.1109/ICRAE48301.2019.9043840

Cho Y, Do HM, Cheong J (2019) Screw based kinematic calibration method for robot manipulators with joint compliance using circular point analysis. Robot Comput Integrated Manufact 60:63–76. https://doi.org/10.1016/j.rcim.2018.08.001

Errandonea I, Beltrán S, and Arrizabalaga S (2020) Digital Twin for maintenance: A literature review. In: Computers in Industry (Vol. 123). Elsevier B.V. https://doi.org/10.1016/j.compind.2020.103316

Foidl H, and Felderer M (2016) Research Challenges of Industry 4.0 for Quality Management, Vol. 245. https://doi.org/10.1007/978-3-319-32799-0_10

Franceschini F, Galetto M, Maisano D, Mastrogiacomo L, Pralio B (2011) Distributed large-scale dimensional metrology. In: Distributed Large-Scale Dimensional Metrology. Springer, London. https://doi.org/10.1007/978-0-85729-543-9

Fu Z, Dai JS, Yang K, Chen X, López-Custodio P (2020) Analysis of unified error model and simulated parameters calibration for robotic machining based on Lie theory. Robot Comput Integrated Manufact. https://doi.org/10.1016/j.rcim.2019.101855

Gan Y, Duan J, Dai X (2019) A calibration method of robot kinematic parameters by drawstring displacement sensor. Int J Adv Robot Syst. https://doi.org/10.1177/1729881419883072

Gao G, Zhang H, San H, Wu X, Wang W (2017) Modeling and error compensation of robotic articulated arm coordinate measuring machines using BP neural network. Complexity. https://doi.org/10.1155/2017/5156264

Gervasi R, Mastrogiacomo L, Franceschini F (2020) A conceptual framework to evaluate human-robot collaboration. Int J Adv Manuf Technol 108(3):841–865. https://doi.org/10.1007/s00170-020-05363-1

Gervasi R, Aliev K, Mastrogiacomo L, Franceschini F (2022) User experience and physiological response in human-robot collaboration: a preliminary investigation. J Intell Robot Syst Theory Appl. https://doi.org/10.1007/s10846-022-01744-8

Giacomo M (2021) Advanced methods for the mechanical and topographical characterization of technological surfaces. Politecnico di Torino.

Gonzalez MK, Theissen NA, Barrios A, Archenti A (2022) Online compliance error compensation system for industrial manipulators in contact applications. Robot Comput Integrated Manufact 76:102305. https://doi.org/10.1016/j.rcim.2021.102305

He B, Bai KJ (2021) Digital twin-based sustainable intelligent manufacturing: a review. Adv Manufact. https://doi.org/10.1007/s40436-020-00302-5

Horn BKP (1984) Extended Gaussian images. Proc IEEE 72:1671–1686

Irino N, Kobayashi A, Shinba Y, Kawai K, Spescha D, Wegener K (2023) Digital twin based accuracy compensation. CIRP Ann. https://doi.org/10.1016/j.cirp.2023.04.088

ISO 23247–1:2021 (2021) Automation systems and integration-Digital twin framework for manufacturing. Part 1: Overview and general principles. ISO, Genève

JCGM 100:2008. Evaluation of measurement data-Guide to the expression of uncertainty in measurement Évaluation des données de mesure-Guide pour l'expression de l'incertitude de mesure. www.bipm.org

Jones D, Snider C, Nassehi A, Yon J, Hicks B (2020) Characterising the digital twin: a systematic literature review. CIRP J Manuf Sci Technol 29:36–52. https://doi.org/10.1016/j.cirpj.2020.02.002

Karl JAM, Wyk V (2016) Simplified framework for robot coordinate registration for manufacturing applications

Khan A, Turowski K (2016) A perspective on industry 4.0: From challenges to opportunities in production systems. In: IoTBD 2016 - Proceedings of the International Conference on Internet of Things and Big Data, 441–448. https://doi.org/10.5220/0005929704410448

Kholkhujaev J, MacUlotti G, Genta G, Galetto M, Inoyatkhodjaev J (2022) Non-contact articulated robot-integrated gap and flushness measurement system for automobile assembly. IEEE Access 10:86528–86541. https://doi.org/10.1109/ACCESS.2022.3199066

Lambrecht J, Kleinsorge M, Rosenstrauch M, Krüger J (2013) Spatial programming for industrial robots through task demonstration. Int J Adv Robot Syst. https://doi.org/10.5772/55640

Lattanzi L, Cristalli C, Massa D, Boria S, Lépine P, Pellicciari M (2020) Geometrical calibration of a 6-axis robotic arm for high accuracy manufacturing task. Int J Adv Manufact Technol 111(7–8):1813–1829. https://doi.org/10.1007/s00170-020-06179-9

Leco M, Kadirkamanathan V (2021) A perturbation signal based data-driven Gaussian process regression model for in-process part quality prediction in robotic countersinking operations. Robot Comput Integrated Manufact. https://doi.org/10.1016/j.rcim.2020.102105

Leco M, McLeay T, Kadirkamanathan V (2022) A two-step machining and active learning approach for right-first-time robotic countersinking through in-process error compensation and prediction of depth of cuts. Robot Comput Integrated Manufact. https://doi.org/10.1016/j.rcim.2022.102345

Li Z, Li S, Luo X (2021) An overview of calibration technology of industrial robots. IEEE/CAA J Automatica Sinica 8(1):23–36. https://doi.org/10.1109/JAS.2020.1003381

Lindström J, Lejon E, Kyösti P, Mecella M, Heutelbeck D, Hemmje M, Sjödahl M, Birk W, Gunnarsson B (2019) Towards intelligent and sustainable production systems with a zero-defect manufacturing approach in an Industry4.0 context. Procedia CIRP 81:880–885. https://doi.org/10.1016/J.PROCIR.2019.03.218

Liu K, Song L, Han W, Cui Y, Wang Y (2022) Time-varying error prediction and compensation for movement axis of CNC machine tool based on digital twin. IEEE Trans Industr Inf 18(1):109–118. https://doi.org/10.1109/TII.2021.3073649

Luo W, Hu T, Ye Y, Zhang C, Wei Y (2020) A hybrid predictive maintenance approach for CNC machine tool driven by Digital Twin. Robot Comput Integrated Manufact. https://doi.org/10.1016/j.rcim.2020.101974

Maculotti G, Genta G, Galetto M (2023) Optimisation of laser welding of deep drawing steel for automotive applications by machine learning: a comparison of different techniques. Qual Reliab Eng Int. https://doi.org/10.1002/qre.3377

Maculotti G, Marschall M, Kok G, Chekh BA, van Dijk M, Flores J, Genta G, Puerto P, Galetto M, Schmelter S (2024) A shared metrological framework for trustworthy virtual experiments and digital twins. Metrology 4(3):337–363. https://doi.org/10.3390/metrology4030021

Mahler J, Krishnan S, Laskey M, Sen S, Murali A, Kehoe B, Patil S, Wang J, Franklin M, Abbeel P, and Goldberg K (n.d.) Learning accurate kinematic control of cable-driven surgical robots using data cleaning and Gaussian process regression

Michael R, Markus L, Markus LP, Manuela W, Pascal E, Michael H and Jan J (2015) Industry 4.0: the future of productivity and growth in manufacturing industries

Nguyen V, Marvel JA (2022) Modeling of industrial robot kinematics using a hybrid analytical and statistical approach. J Mechan Robotics. https://doi.org/10.1115/1.4053734

OptiTrack - Motive - In Depth. (n.d.). Retrieved November 2, 2023, from https://optitrack.com/software/motive/

Oyekan JO, Hutabarat W, Tiwari A, Grech R, Aung MH, Mariani MP, López-Dávalos L, Ricaud T, Singh S, Dupuis C (2019) The effectiveness of virtual environments in developing collaborative strategies between industrial robots and humans. Robot Comput Integrated Manufact 55:41–54. https://doi.org/10.1016/j.rcim.2018.07.006

Oztemel E, Gursev S (2020) Literature review of Industry 4.0 and related technologies. J Intell Manufact 31(1):127–182. https://doi.org/10.1007/s10845-018-1433-8

Peshkin M, and Colgate JE (n.d.). Cobots. http://www2.mcb.co.uk/mcbrr/ir.asp

Posada JRD, Schneider U, Pidan S, Geravand M, Stelzer P and Verl A (2016) High accurate robotic drilling with external sensor and compliance model-based compensation. In: 2016 IEEE International Conference on Robotics and Automation (ICRA), 3901–3907. https://doi.org/10.1109/ICRA.2016.7487579

Pottier C, Petzing J, Eghtedari F, Lohse N, Kinnell P (2023) Developing digital twins of multi-camera metrology systems in Blender. Measure Sci Technol. https://doi.org/10.1088/1361-6501/acc59e

Rasmussen CE (2003) LNAI 3176 - Gaussian Processes in Machine Learning. In LNAI (Vol. 3176). Springer-Verlag. http://www.tuebingen.mpg.de/~carl

ISO/TS 15066:2016. (2016) Robots and robotic devices—Collaborative robots. BSI Standards Publication.

Rosen R, Von Wichert G, Lo G, Bettenhausen KD (2015) About the importance of autonomy and digital twins for the future of manufacturing. IFAC-PapersOnLine 28(3):567–572. https://doi.org/10.1016/j.ifacol.2015.06.141

Salkin C, Oner M, Ustundag A, Cevikcan E (2018) A conceptual framework for industry 4.0. In: Ustundag A, Cevikcan E (eds) Industry 4.0: managing the digital transformation. Springer, Berlin, pp 3–23. https://doi.org/10.1007/978-3-319-57870-5_1

Sanderud A, Thomessen T, Osumi H, Niitsuma M (2015) A proactive strategy for safe human-robot collaboration based on a Simplified risk analysis. MIC Model Identif Control 36(1):11–21. https://doi.org/10.4173/mic.2015.1.2

Santolaria J, Conte J, Ginés M (2013) Laser tracker-based kinematic parameter calibration of industrial robots by improved CPA method and active retroreflector. Int J Adv Manufact Technol 66(9):2087–2106. https://doi.org/10.1007/s00170-012-4484-6

Saravanan A, Jerald J, Rani DCA (2020) An intelligent constitutive and collaborative framework by integrating the design, inspection and testing activities using a cloud platform. Int J Comput Integrated Manufact 33(5):440–459. https://doi.org/10.1080/0951192X.2020.1736712

Shanghai BH, Shanghai WD and Yu T (2021) Research on positioning error compensation of industrial robot based on BP neural network. In: 2021 International Conference on Information Science, Parallel and Distributed Systems (ISPDS), 131–135. https://doi.org/10.1109/ISPDS54097.2021.00033

Shu T, Gharaaty S, Xie W, Joubair A, Bonev IA (2018) Dynamic path tracking of industrial robots with high accuracy using photogrammetry sensor. IEEE/ASME Trans Mechatron 23(3):1159–1170. https://doi.org/10.1109/TMECH.2018.2821600

Slavkovic N, Zivanovic S, Kokotovic B, Dimic Z, Milutinovic M (2020) Simulation of compensated tool path through virtual robot machining model. J Brazil Soc Mechan Sci Eng. https://doi.org/10.1007/s40430-020-02461-9

Song Y, Liu M, Lian B, Qi Y, Wang Y, Wu J, Li Q (2022) Industrial serial robot calibration considering geometric and deformation errors. Robot Comput Integrated Manufact. https://doi.org/10.1016/j.rcim.2022.102328

Tao F, Cheng J, Qi Q, Zhang M, Zhang H, Sui F (2018) Digital twin-driven product design, manufacturing and service with big data. Int J Adv Manuf Technol 94(9–12):3563–3576. https://doi.org/10.1007/s00170-017-0233-1

Tsarouchi P, Matthaiakis AS, Makris S, Chryssolouris G (2017) On a human-robot collaboration in an assembly cell. Int J Comput Integr Manuf 30(6):580–589. https://doi.org/10.1080/0951192X.2016.1187297

Verna E, Puttero S, Genta G, Galetto M (2023) Toward a concept of digital twin for monitoring assembly and disassembly processes. Quality Eng. https://doi.org/10.1080/08982112.2023.2234017

Verna E, Puttero S, Genta G, Galetto M (2023a) A novel diagnostic tool for human-centric quality monitoring in human-robot collaboration manufacturing. J Manufact Sci Eng. https://doi.org/10.1115/1.4063284

Verna E, Puttero S, Genta G, Galetto M (2023b) Exploring the effects of perceived complexity criteria on performance measures of human-robot collaborative assembly. J Manufact Sci Eng. https://doi.org/10.1115/1.4063232

Wang D, and Bai Y (2005) Improving position accuracy of robot manipulators using neural networks

Wilhelm J, Beinke T and Freitag MJ (2020) Improving human-machine interaction with a digital twin

Wu L, Yang X, Chen K, Ren H (2015) A minimal POE-based model for robotic kinematic calibration with only position measurements. IEEE Trans Autom Sci Eng 12(2):758–763. https://doi.org/10.1109/TASE.2014.2328652

Wu J, Wu H, Song Y, Zhang T, Zhang J, Cheng Y (2018) Adaptive Neuro-fuzzy inference system based estimation of EAMA elevation joint error compensation. Fusion Eng des 126:170–173. https://doi.org/10.1016/j.fusengdes.2017.11.025

Wu Z, Chen S, Han J, Zhang S, Liang J, Yang X (2022) A low-cost digital twin-driven positioning error compensation method for industrial robotic arm. IEEE Sens J 22(23):22885–22893. https://doi.org/10.1109/JSEN.2022.3213428

Yin Y, Stecke KE, Li D (2018) The evolution of production systems from Industry 2.0 through Industry 4.0. Int J Product Res 56(1–2):848–861. https://doi.org/10.1080/00207543.2017.1403664

Zhang Z, Malashkhia L, Zhang Y, Shevtshenko E, Wang Y (2022) Design of Gaussian process based model predictive control for seam tracking in a laser welding digital twin environment. J Manuf Process 80:816–828. https://doi.org/10.1016/j.jmapro.2022.06.047

Zhao H-N, Yu L-D, Jia H-K, Li W-S, Sun J-Q (2016) A new kinematic model of portable articulated coordinate measuring machine. Appl Sci. https://doi.org/10.3390/app6070181

Zhou J, Zheng L, Fan W, Zhang X, Cao Y (2023) Adaptive hierarchical positioning error compensation for long-term service of industrial robots based on incremental learning with fixed-length memory window and incremental model reconstruction. Robot Comput Integrated Manufact 84:102590. https://doi.org/10.1016/j.rcim.2023.102590

Zhu Z, Lin Z, Huang J, Zheng L, He B (2023) A digital twin-based machining motion simulation and visualization monitoring system for milling robot. Int J Adv Manufact Technol 127(9–10):4387–4399. https://doi.org/10.1007/s00170-023-11827-x

Giacomo Maculotti received the Master of Science Degree in Automotive Engineering in 2017 and the PhD Degree in "Management, Production and Design" in 2020 from Politecnico di Torino, Italy. He is currently an assistant Professor at Politecnico di Torino - Dept. of Management and Production Engineering (DIGEP), where he teaches "Mechanical and topographical characterization of technological surfaces" and "Experimental Statistics and Mechanical Measurement". His current research interests are Industrial Metrology, Technological Surfaces Characterization, and Quality Engineering, with particular focus on traceable digital twin and the development of measurement systems.

Fazluddin Khusnuddinov received his Master of Science degree in Mechatronics Engineering in 2017 from the Turin Polytechnic University in Tashkent, Uzbekistan. He is currently an assistant lecturer and a PhD student at the Turin Polytechnic University in Tashkent. His current research interests include machine vision, mechatronic systems, collaborative robotics, Industry 4.0/5.0, and digital twins for industry.

Jasurkhuja Kholkhujaev received the Master of Science Degree in Mechatronics Engineering in 2017, Turin Polytechnic University in Tashkent, Uzbekistan, and the PhD Degree in "Management, Production and Design" in 2023 from Politecnico di Torino, Italy. He is currently postdoctoral researcher at Department of Mechanical and Aerospace engineering in Turin polytechnic university in Tashkent. His current research interests are Visual Inspection, Industrial Metrology, Machine Vision, and Quality Engineering.

Gianfranco Genta received the Master of Science Degree in Mathematical Engineering from Politecnico di Torino, Italy, in 2005 and the PhD Degree in "Metrology: Measuring Science and Technique" from Politecnico di Torino in 2010. He is currently Associate Professor at the Department of Management and Production Engineering (DIGEP) of the Politecnico di Torino, where he teaches "Design of industrial experiments", "Experimental Statistics and Mechanical Measurement", and "Quality and measurements management lab". He is an Associate Member of CIRP (The International Academy for Production Engineering) and Fellow of A.I.Te.M. (Associazione Italiana di Tecnologia Meccanica). He is author and coauthor of 3 books and more than 70 publications on international journals and conference proceedings. His current research focuses on Industrial Metrology, Quality Engineering and Experimental Data Analysis.

Maurizio Galetto received the Master of Science Degree in Physics from University of Turin, Italy, in 1995 and the PhD Degree in "Metrology: Measuring Science and Technique" from Politecnico di Torino, Italy, in 2000. He is currently Full Professor and Head of the Department of Management and Production Engineering (DIGEP) of the Politecnico di Torino, where he teaches "Quality Engineering" and "Experimental Statistics and Mechanical Measurement". He is Associate Member of CIRP (The International Academy for Production Engineering) and Fellow of A.I.Te.M. (Associazione Italiana di Tecnologia Meccanica) and E.N.B.I.S. (European Network for Business and Industrial Statistics). He is Member of the Editorial Board of the scientific international journal Nanomanufacturing and Metrology and collaborates as referee for many international journals in the field of Industrial Engineering. He is author and coauthor of 4 books and more than 100 published papers in scientific journals, and international conference proceedings. His current research interests are in the areas of Quality Engineering, Statistical Process Control, Industrial Metrology and Production Systems. At present, he collaborates in some important research projects for public and private organizations.